Ecological Indicators 137 (2022) 108790

Contents lists available at ScienceDirect

Ecological Indicators

journal homepage: www.elsevier.com/locate/ecolind

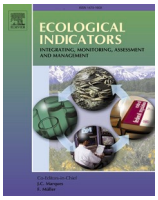

Original Articles

HABs in coastal upwelling systems: Insights from an exceptional red tide of the toxigenic dinoflagellate *Alexandrium minutum*

E. Nogueira [a], I. Bravo [a], P. Montero [b], P. Díaz-Tapia [c], S. Calvo [b], B. Ben-Gigirey [a,1], R. I. Figueroa [a], J.L. Garrido [d], I. Ramilo [a], N. Lluch [a], A.E. Rossignoli [a,2], P. Riobó [d], F. Rodríguez [a,*]

[a] Centro Nacional Instituto Español de Oceanografía (IEO-CSIC), Centro Oceanográfico de Vigo, 36390 Vigo, Spain
[b] Instituto Tecnolóxico para o Control do Medio Mariño de Galicia, 36611 Vilagarcía de Arousa, Spain
[c] Centro Nacional Instituto Español de Oceanografía (IEO-CSIC), Centro Oceanográfico de A Coruña, 15001 A Coruña, Spain
[d] Instituto de Investigaciones Marinas, Consejo Superior de Investigaciones Científicas (IIM-CSIC), 36208 Vigo, Spain

ARTICLE INFO

Keywords:
Alexandrium minutum
Time-series
Model simulations
Galician Rías
NW Iberian Peninsula
Paralytic shellfish poisoning
Harmful algal bloom

ABSTRACT

Alexandrium minutum blooms generally occur in semi-enclosed sites such as estuaries, harbours and lagoons, where enhanced stratification, restricted circulation and accumulation of resting cysts in the sediment set suitable habitat conditions for the proliferation of this paralytic shellfish poisoning toxigenic species. In the Galician Rías Baixas (NW Iberian Peninsula), according to weekly time-series between 1994 and 2020, blooms of *A. minutum* were recurrent in small, shallow estuarine bays inside the Rías de Vigo and Pontevedra, but rarely detected, and if so at low concentrations, out of these environments. However, from May to July 2018 it developed as usual in the small inner bays but then spread over both Rías (Vigo and Pontevedra) causing discoloured waters during one month and prolonged harvesting closures. Meteorological conditions during that period (rains / runoff higher than climatological averages, sustained temperature increment and oscillating wind pattern –i.e., series of upwelling-relaxation cycles), fostered optimal circumstances for the development of that extensive and massive proliferation: strong vertical stratification and the alternation of retention and dispersion processes. Simulations from a particle tracking model portrayed the observed bloom development phases: onset and development inside a small inner bay; transport within the surface layer, from these sites towards the interior parts of the Ría; and dispersion all over the embayment. Seedbeds with high concentrations of resting cysts were detected several months after the bloom, which may have favoured flourishment of *A. minutum* in the following two years, markedly in 2020. The present work contributes to the general understanding of the dynamics of harmful algal blooms (HABs), from which surveillance indicators of the state of marine ecosystems and their evolution can be derived. We hypothesize that the intensity and frequency of *A. minutum* proliferations in the Galician Rías could increase under projected climate trends.

1. Introduction

Harmful Algal Blooms (HABs) are recurrent episodes in open oceans and coastal waters, that impact ecosystem status and affect recreational and aquaculture activities inducing considerable economic losses (Gessner 2000; Hallegraeff 2010; Anderson 2014). The current global warming scenario appears to be, among other causes, behind the geographical expansion of HABs and the apparent increase in their occurrence and persistence (Hallegraeff 2010; Gobler et al., 2017), though intensified monitoring and bloom impacts have been argued to play an important role in these observed trends (Hallegraeff et al., 2021). The effect of warming on HABs dynamics remains difficult to assess due to temperature interactions with other physical, chemical and biological drivers (Tester et al., 2020; Wells et al., 2020).

The Galician coast (NW Iberian Peninsula) is indented by natural flooded tectonic valleys called “Rías”. The region is located at the

Abbreviations: HAB, Harmful Algal Bloom; PSP, Paralytic Shellfish Poisoning.

* Corresponding author.
E-mail address: francisco.rodriguez@ieo.csic.es (F. Rodríguez).
[1] Present address: European Union Reference Laboratory for Marine Biotoxins, Citexvi Campus Universitario de Vigo, 36310, Vigo, Spain.
[2] Present address: Centro de Investigacións Mariñas (CIMA), 36620, Vilanova de Arousa, Spain.

https://doi.org/10.1016/j.ecolind.2022.108790
Received 28 January 2022; Received in revised form 16 March 2022; Accepted 17 March 2022
Available online 22 March 2022

northern boundary of the Canary Current Upwelling System (Arístegui et al., 2009). The occurrence of seasonal upwelling events, mainly from spring to autumn, favours high productivity and phytoplankton biomass in the Rías, supporting an intensive aquaculture and fishery industry (shellfish growth in rafts and harvesting of precious molluscs and crustaceans). Active growth and/or passive accumulation inside the Rías also drive the periodical occurrence of HABs (Álvarez-Salgado et al., 2008; Díaz et al., 2016), posing risk for public health and socioeconomic damage due to shellfish harvesting closures. The NW Iberian Peninsula has experienced, following global trends, a significant increase in land and sea surface temperatures since 1974 (Gómez-Gesteira et al., 2011). Trends and anomalies in climate conditions may affect the prevalence and intensity of HABs, as suggest for instance the longer shellfish harvesting bans in the Rías Baixas parallel to weakening of coastal upwelling in the NW Iberian shelf over the last decades (Álvarez-Salgado et al., 2008; Pérez et al., 2010).

The occurrence of discoloured waters in the Galician Rías was well-known since more than hundred years by seafarers, who named the events as "*purga do mar*" ("purge of the sea"; Sobrino 1918). The first mention in the literature dates back to summer 1916 in the Ría de Vigo (RV) (de Buen 1916). By then, radiolarians were erroneously suggested as the causative agents, but the following year the dinoflagellate *Gonyaulax polyedra* (=*Lingulodinium polyedra*; Sobrino, 1918) was unambiguously identified as responsible for red tides in the area. Later on, Margalef (1956) provided the first detailed study about red tides in Galicia (RV) due to dinoflagellates (*G. spinifera* and *G. polyedra*) and the ciliate *Mesodinium rubrum*.

Oceanographic dynamics inside the Galician Rías, modulated mainly by a predominant positive residual circulation pattern driven by buoyancy currents (estuarine character) and the seasonal occurrence of upwelling events (shelf-coastal interactions), often hinder the formation of extensive and prolonged red tides (Reguera et al. 2008). Nonetheless, under calm weather conditions in spring and summer, discoloured waters develop sporadically. In the last decades, most registered red tides have been caused by non-toxic species of the heterotrophic dinoflagellate *Noctiluca scintillans* and the photosynthetic ciliate *Mesodinium rubrum*. To our knowledge, the only exceptions were the toxic proliferations of the dinoflagellate *Gymnodinium catenatum* in 1976 and 1986 in the Rías Baixas (Fraga, 1989; Reguera et al., 2008; Rodríguez 2017), and a paralytic shellfish poisoning (PSP) outbreak in the northern Ría de Ares in 1984 by *Alexandrium minutum* (reported as *Gonyaulax tamarensis*; Blanco et al., 1985).

Alexandrium minutum is a global distributed species with variable toxin profiles and potential impact for human health and aquaculture activities, despite a few records of non-toxic populations (Lewis et al., 2018). Its proliferations are mainly observed in sheltered coastal areas (harbours, estuaries or embayments), but the environmental and biological factors contributing to the initiation of *A. minutum* blooms are different in each geographical area (Lewis et al., 2018). This knowledge is of paramount importance in order to develop predictive tools and monitor its regional development for better management decisions during toxic outbreaks. Blooms of *A. minutum* have been typically detected from late spring to summer inside small, shallow estuarine bays such as Ría de Ares in the northern Rías Altas, and Baiona (RV) and Aldán (Ría de Pontevedra, RP) in the southern Rías Baixas. These blooms occur associated to strong vertical haline / thermal gradients and low-moderate dispersion (Blanco et al., 1985; Bravo et al., 2010a), attaining maximum concentrations around 10^5 cells L^{-1} (Bravo et al., 2010a).

The present study addresses an exceptional PSP outbreak in the Rías Baixas (RV and contiguous northward RP) from May to July 2018, associated with an intense and prolonged red tide (~1 month), and the environmental conditions that favoured its development. Description of the spatial and temporal dynamics of the bloom, from its onset to decay, was based on time series analysis of data from the regular HAB monitoring (INTECMAR; weekly from 1994 to 2020 at a grid of stations), opportunistic sampling during the bloom, and cyst mapping in sediments of the affected area several months after the red tide. The bloom causative organism, *A. minutum*, and the community ensemble was characterised combining morphological, pigment and molecular analyses (epifluorescence light microscopy, HPLC, ITS rDNA sequencing and metabarcoding of the V4 region of the 18S gene). Analysis of ancillary meteorological and hydrographic time series and simulations from a particle tracking model were applied to assess the primary drivers of the observed bloom dynamics. The consequences of this event for the proliferation of *A. minutum* in the Rías Baixas in the following years, and the potential positive link with climate change in the area are discussed.

2. Material and methods

2.1. *Alexandrium sp. cell counts and environmental data from time-series monitoring programmes*

Weekly reports of cell abundances of *A. minutum* (labelled as *Alexandrium* sp.) between 1994 and 2020 in RV and RP (Fig. 1A) were obtained from the HAB monitoring programme of Instituto Tecnolóxico para o Control do Medio Mariño de Galicia (INTECMAR, https://www.intecmar.gal; Xunta de Galicia) (grid of stations in Fig. 1C). These samples were collected using a PVC hose (Lindahl, 1986) divided in three sections: 0–5, 5–10 and 10–15 m. Then, those sections were pooled into an integrated sample for phytoplankton cell counts (0–15 m). The only exception to this procedure is station G0 (Baiona), where surface seawater was collected with a bucket. Seawater samples were then preserved in Lugol's iodine (LI) solution, and sedimented in Utermöhl's chambers (25 ml) for at least 12 h. Cell counts were obtained using an inverted microscope (Nikon Diaphot TMD). The whole bottom of the chamber was examined at 100 × magnification to identify the largest organisms, and diametral transects at 200 × and 400 × aided to identify the smallest and usually more abundant organisms.

Hydrographic conditions during the bloom (1st May to 31st July) were inferred from temperature and salinity profiles (CTD SBE25) at the monitoring stations (INTECMAR; Fig. 1C). Meteorological data (air temperature, rainfall, daily irradiance and wind direction and intensity) were retrieved from MeteoGalicia (Port of Vigo station; https://www.meteogalicia.gal/) and the European Climate Assessment & Dataset (ECAD; Vigo-Peinador station; https://www.ecad.eu/). Upwelling index time series were downloaded from the Spanish Oceanographic Institute (historical FNMOC data series; https://www.indicedeafloramiento.ieo.es/). Freshwater inputs in RV were obtained from the legal entity for water management (Augas de Galicia) as displayed in MeteoGalicia website for the main rivers (Groba, Miñor, Lagares, Oitavén-Verdugo).

2.2. *Red tide sampling*

Sampling of discoloured waters was carried out at seven sampling sites in RV (Fig. 1B; Table 1). The occurrence of an extensive red tide was reported by first aid and rescue services at Samil beach in the morning of June 28th 2018. Seawater samples were then taken near the shoreline using an Apstein-like net (20 μm mesh-size) revealing a nearly monospecific bloom of *Alexandrium minutum* (see 2.4. and results section).

During subsequent dates up to the end of July, red waters were observed moving back and forth along the Vigo marina and several locations in RP (Supplementary Material S1). Surface seawater samples for the isolation of *A. minutum* strains, pigment analysis and cell counts were collected with a bucket at seven sampling sites at the red tide in RV (labelled 1 to 7 in Fig. 1B inset; Table 1). In addition, high vertical resolution profiles were obtained at the surface layer with a hose (135 cm length, divided into eight sections of 15 cm). The hose was deployed by hand in sampling site 2 (Vigo marina, dockyards) (Supplementary Material S1E). In those samples, cell counts of *A. minutum* were performed after LI fixation, diluted with filtered seawater and enumerated using a Sedgwick-Rafter chamber. Field samples (15–50 ml) for pigment analyses by HPLC were filtered through 4.7 cm diameter GF/F glass

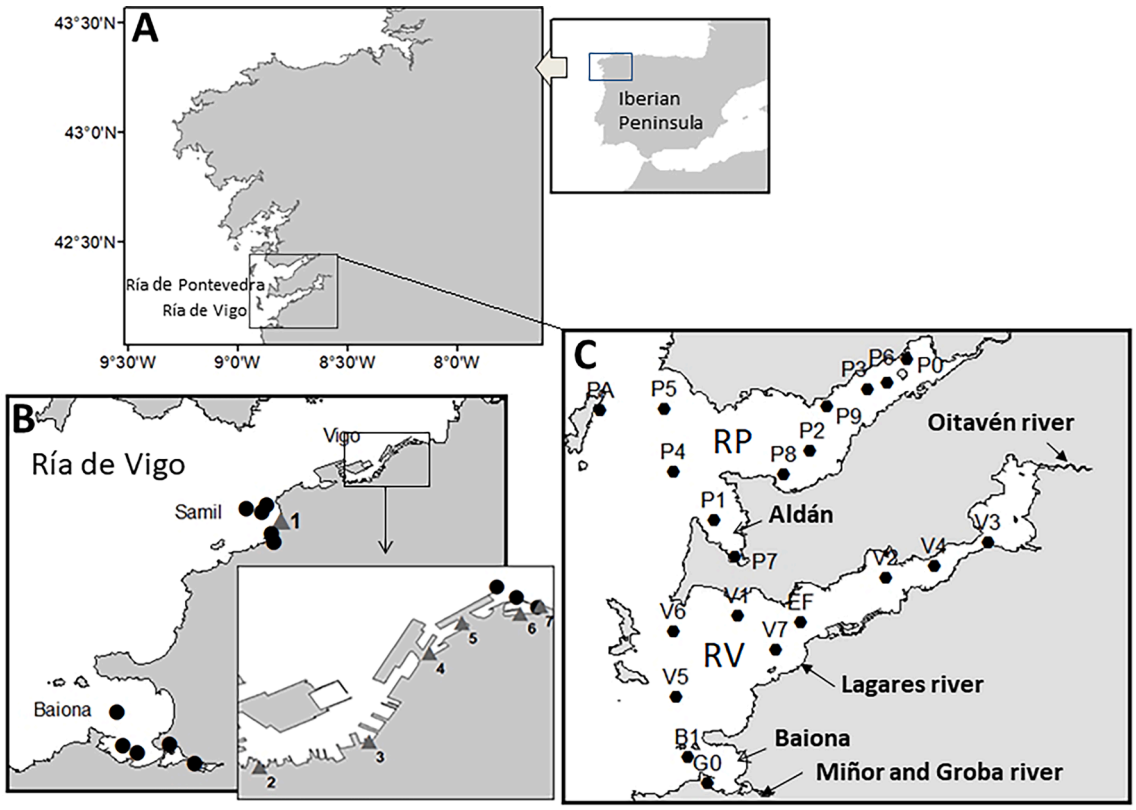

Fig. 1. Study area and observations. (A) Northern limit of the Canary Current Upwelling System and Rías Baixas; (B) Sampling stations for cyst mapping (black circles) and seawater samples from red tide waters (triangles) in the Vigo marina and Samil beach; (C) Sampling stations grid of the Galician HAB monitoring programme (INTECMAR -https:\\www.intecmar.gal) in the Rías de Vigo (RV) and Pontevedra (RP).

Table 1
Sampling locations for phytoplankton (water column) and cysts (sediments), as depicted in Fig. 1B (numbered triangles and black circles, respectively). Sediment sites were pooled out as replicates and numbered according with five locations.

Sampling site	Coordinates
Water column	
1: Samil beach	42°12′38.0″N, 8°46′34.3″W
2: Vigo marina (dockyards)	42°13′32.2″N, 8°44′57.2″W
3: Vigo marina (Beiramar)	42°13′41.5″N, 8°44′17.2″W
4: Vigo marina (inshore pier)	42°14′13.9″N, 8°43′55.0″W
5: Vigo marina (A Laxe)	42°14′25.1″N, 8°43′43.2″W
6: Vigo marina (Náutico)	42°14′28.5″N, 8°43′21.7″W
7: Vigo marina (As Avenidas)	42°14′31.1″N, 8°43′14.4″W
Sediment	
B1: Baiona bay	42° 8′ 4.4″N, 8° 50′ 28.7″W
B2: Baiona bay	42° 7′ 6.4″N, 8° 49′ 58.7″W
B3: Baiona bay	42° 7′ 16.6″N, 8° 50′ 19.7″W
M1: Miñor estuary	42° 6′ 49.9″N, 8° 48′ 36.5″W
M2: Miñor estuary	42° 7′ 17.1″N, 8° 49′ 12.7″W
SA1: Samil beach	42° 12′ 55.1″N, 8° 47′ 23.8″W
SA2: Samil beach	42° 12′ 50.7N“, 8° 47′ 1.8″W
SA3: Samil beach	42° 13′ 1.3″N, 8° 46′ 54.7″W
LA1: Lagares estuary	42° 12′ 8.3″N, 8° 46′ 44.1″W
LA2: Lagares estuary	42° 12′ 18.9″N, 8° 46′ 47.8″W
VG1: Vigo marina (As Avenidas)	42° 14′ 38.24″N, 8° 43′ 30.2″W
VG2: Vigo marina (As Avenidas)	42° 14′ 34.2″N, 8° 43′ 23.0″W
VG3: Vigo marina (As Avenidas)	42° 14′ 30.7″N, 8° 43′ 15.4″W

microfiber filters (nominal pore size 0.7 μm, Whatman, Sigma-Aldrich, Maidstone, UK), with a vacuum pump under low pressure. Filters were frozen and kept at − 40 °C until further analysis, following Zapata et al. (2000).

Single *A. minutum* cells were isolated using a glass capillary pipette and poured into 96-microwell plates in L1 medium (Guillard and Hargraves, 1993) without silicates, made with seawater from RV and salinity adjusted to 32. Plates were incubated at 19 °C with a photon irradiance of about 120 μmol m^{-2} s^{-1} of PAR (LED illumination), measured with a QSL-100 irradiometer (Biospherical Instruments Inc., San Diego, CA, USA) and at a 12:12 L:D photoperiod. The obtained clonal cultures were maintained in 50 ml Erlenmeyer flasks for further toxinological characterization (Ben-Gigirey et al., 2020) and strain S1, isolated on June 28th in Samil beach (sampling site 1, Fig. 1B; Table 1), was used for detailed identification and characterisation (see 2.4.). Furthermore, two bloom samples were incubated in PYREX® 5 L bottles (same culture conditions as above), in order to check if there was a significant population encystment (resting cyst formation) following nutrient depletion, a fact that would indicate a high number of sexual zygotes in the original sample.

2.3. Cyst mapping

In order to study cyst distribution in RV, sediment samples were collected from 13 stations (Fig. 1B; Table 1) in March 2019. Three samples separated from each other approximately 50 m were taken at each station. Samples were collected by a scuba diver placing plastic cylinders of 10 cm long and 3 cm base diameter into the sediment. In order to avoid the loss of cysts in the uppermost sediment layer, the water over the sediment was also sampled and brought to the laboratory taking care of keeping sampling containers upright. Samples were stored in darkness and at 4 °C temperature. The first centimetre of the sediment was processed within 1 month from sampling by means of sieving and density gradient following Bravo et al. (2006). Resting cysts of *A. minutum* were counted in subsamples (1–3 ml) placed in an Utermöhl sedimentation chamber using a Zeiss Axiovert 135 inverted microscope

at 400 × magnification. The cysts were identified following the description in Bravo et al. (2010b). Fifteen cysts were isolated as described in section 2.1, five of which germinated and the resulting vegetative cells were studied to ensure that the cysts had been correctly identified.

2.4. Identification and characterization of A. minutum from the bloom

Bloom responsible organism, *A. minutum* (strain S1), was identified morphologically by epifluorescence light microscopy using a Leica DMLA light microscope (Leica Microsystems GmbH, Wetzlar, Germany). Plate pattern identification of the cells was performed after staining with Fluorescent Brightener 28 (Sigma–Aldrich, St. Louis, MO, USA) following Fritz and Triemer (1985).

For the molecular characterization of strain S1, 10 cells were picked with a glass micropipette, washed in milli-Q water and placed in a 200 µl microtube. Liquid nitrogen cold shocking was applied and samples kept at −20 °C before PCR analysis. The internal transcribed spacer (ITS1 and ITS2) and 5.8S rRNA gene regions were amplified in a Surecycler 8800 thermocycler using the pairs of primers ITSF01/PERK-ITS-AS (Ki & Han 2007; Kotob et al., 1999). PCR conditions followed Nascimento et al. (2017). PCR products were purified with ExoSAP–IT (USB, Cleveland, OH, USA), sequenced using the Big Dye Terminator v.3.1 reaction cycle sequencing kit (Applied Biosystems, Foster City, CA, USA), and separated on an AB 3130 sequencer (Applied Biosystems; CACTI sequencing facilities of the University of Vigo, Spain). The ITS sequence (597 nucleotides, including flanking regions of SSU, LSU and full length ITS rDNA) obtained was deposited in the GenBank database (Acc. No. MT627441).

2.5. Metabarcoding analyses

Samples for metabarcoding (and complementary pigment) analyses of the bloom were collected at the surface layer in sampling sites 2, 4 and 7 (Fig. 1B inset). A fourth sample was collected with a bucket just outside the Vigo marina dockyard (~50 m from sampling site 7). A volume of ~ 150 ml was filtered with a vacuum pump through a Nuclepore 5 µm pore-size nitrocellulose filter and frozen as detailed previously for pigment analyses. Total DNA was extracted following a phenol–chloroform protocol (Massana et al., 1997) with slight modifications (Guerrero-Feijóo et al., 2017). The V4 region of the 18S rRNA gene was amplified using the primer pairs TAReuk454FWD1 and V4_18S_Next.Rev PCR (Stoeck et al., 2010; Piredda et al., 2017). Reactions were performed in a total volume of 20 µl consisting of 2 µl 10 × reaction buffer, 1 µl 10 µM of forward and reverse primers, 0.4 µl 10 mM dNTPs, 0.6 µl 50 mM $MgCl_2$, 0.25 µl 5 U/µl Taq DNA Polymerase (Roche, Switzerland), 0.5 µl of 20 mg/ml BSA, 13.25 µl MiliQ® water and 1 µl template DNA. PCR cycling profile comprised an initial activation step at 95 °C for 5 min, followed by 10 three-step cycles consisting of 94 °C for 30 s, 62 °C for 45 s, and 72 °C for 1 min, which was followed by 25 further cycles consisting of 94 °C for 30 s, 47 °C for 45 s, and 72 °C for 1 min; and a final 2 min extension at 72 °C. Library preparation was carried out by AllGenetics & Biology SL and sequenced using Illumina MiSeq PE300.

Paired Illumina reads were initially processed using *cutadapt* (Martin 2011) to trim primers and spurious sequences. Amplicon sequence variants (ASVs) were differentiated using DADA2 (Callahan et al., 2016) implemented in R (R Core Team, 2020). Sequences were aligned against PR2 version 4.12.0 and SILVA 132 18S rRNA databases as references (Guillou et al., 2013; Morien and Parfrey, 2018). Illumina MiSeq sequences have been deposited in the National Center for Biotechnology Information (NCBI) Sequence Read Archive (SRA) under bioproject number (PRJNA818162). We constructed an ASVs table after rarefaction of ASVs using the *vegan* package in R and considering the lowest amount of reads (32292).

2.6. Particle (passive) tracking model

The effect of hydrodynamic variability on *A. minutum* bloom dynamics was explored with a particle tracking model adapted to the studied area. The Lagrangian (particle tracking) model (Leitão, 1996) used in the present study belongs to the MOHID modelling system (Martins et al., 2001; Braunschweig et al., 2004). The model has been applied to study several subjects, such as dispersion of pollutants (Gómez-Gesteira et al., 1999), oil spill forecasting (Carracedo et al., 2006) and marine litter tracking (Declerck et al., 2019).

In the model, particle velocity and direction are the result of advection and turbulence processes. The advection contribution is forced by the results of MeteoGalicia hydrodynamic system. This operational system runs daily the MOHIDWater model (https://mohid.com) (Martins et al., 2001) for the simulation of currents, salinity and temperature fields in RV. The horizontal resolution of the hydrodynamic model is 300 × 300 m. Vertical discretization consists of two domains with an interface at 8.68 m. The bottom domain has 16 z-level layers, and the surface domain 11 sigma layers that permit the resolution needed to describe the effect of wind forcing in the surface layer. Surface boundary condition are imposed by WRF (Weather Research and Forecasting Model) applied to Rías Baixas area with a spatial step of 1.3 km. This model is operationally run by MeteoGalicia. A detailed description of model implementation on this domain is found in Huhn et al. (2012) and Venâncio et al. (2019). In addition, the model is forced by the discharges of the Verdugo-Oitavén river through the SWAT model, and the influence at the open ocean boundary from velocity, temperature, and salinity fields predicted by the nested ROMS coastal model, also included in the MeteoGalicia prediction system. The effect of turbulence on particle trajectories is simulated by a random walk approach (Allen, 1982).

The modelled particles were forced to remain in the surface layer of the model, since the interest is to track water parcels of the surface layer, the habitat of *A. minutum* (section 3.1.2). The direct effect of the wind on the particles was not considered. Therefore, modelled Lagrangian tracers are representative of parcels of water with neutral buoyancy within the top few centimetres of the water column. Although the Lagrangian model is not forced directly by the wind, due to the high discretization of the surface layers (the maximum width of the top layer is 11 cm) most of this influence is collected by the surface boundary layer of the hydrodynamic model. Particles moving out of the domain were eliminated. The slipping condition was imposed for the lateral boundary in the coastline.

To simulate the dynamics of *A. minutum* inferred from observations, the particle tracking model was run for two different modelling conditions (named case 1 and 2) mimicking different bloom development stages (section 3.1.). In case 1, model runs simulate the bloom onset in Baiona Bay and its dispersion from there to RV. To model cell growth in the small embayment, a particle emission box corresponding to the Baiona Bay area was defined, and 50 Lagrangian tracers were released within it every 6 h. After that, particle tracking represents the transport of cells as passive tracers. This simulation is performed for the period between May 25th and July 23rd. In case 2, model runs simulate the spread of *A. minutum* once the population is already on the south shoreline margin of RV. To this aim, two zones of possible emission were created: box 1, including Samil beach and the Port of Vigo, and box 2, corresponding to the cove of Chapela (between V3 and V4 INTECMAR stations; Fig. 1C). As before, these boxes emit 50 particles every 6 h, which are dragged by the surface current. The simulation period runs from June 6 to July 23.

3. Results

3.1. Bloom dynamics of *A. minutum* from observations

3.1.1. Historical records

Time series of cell abundance (from January 1994 to December 2020) show that *A. minutum* has been irregularly present in RV (Fig. 2) and RP (Supplementary Material S2). When detected, it was observed seasonally from May to October mainly in Baiona Bay (RV, St. B1 and G0) and Aldán (RP, St. P7). High values where reached occasionally (e.g. $2.3{\cdot}10^6$ cells·L^{-1} in G0, August 6th 1998), but low to moderate abundances (10^3-10^5 cell·L^{-1}), mostly in Baiona Bay between 1998 and 2006, were the norm until the 2018 bloom (section 3.1.2) and following years: 2019 was also atypical since *A. minutum* was early detected on February 18th in RP (St. P0) and in March 11th in Baiona Bay, where reached maximum concentrations in June, and in 2020, *A. minutum* appeared

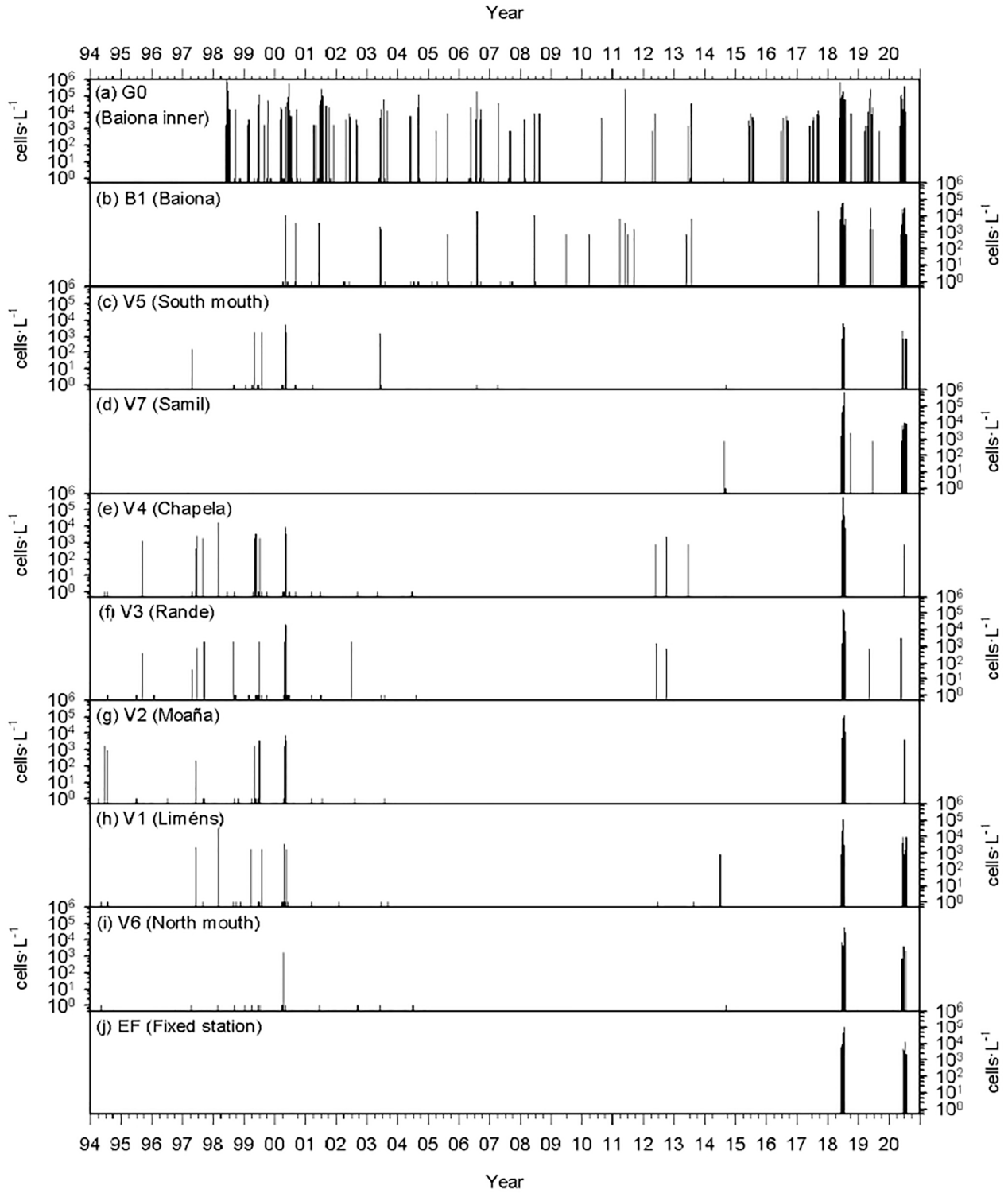

Fig. 2. Time series of *A. minutum* cell abundance (cells·L^{-1}), weekly from January 1994 to December 2020 in the Ría de Vigo from INTECMAR (https:\\www.intecmar.gal). (Suppl. Mat. S2 for Ría de Pontevedra -RP). See Fig. 1C for sampling site codes.

since April through July in high numbers in the Rías Baixas (both in RV and RP) reaching maxima abundances also in June.

3.1.2. The 2018 bloom

In 2018, *A. minutum* was first detected (bloom onset) by the monitoring programme around mid-May inside Baiona Bay (station G0), where it reached the maximum abundance (ca. $7{\cdot}10^5$ cells$\cdot$L^{-1}) on May

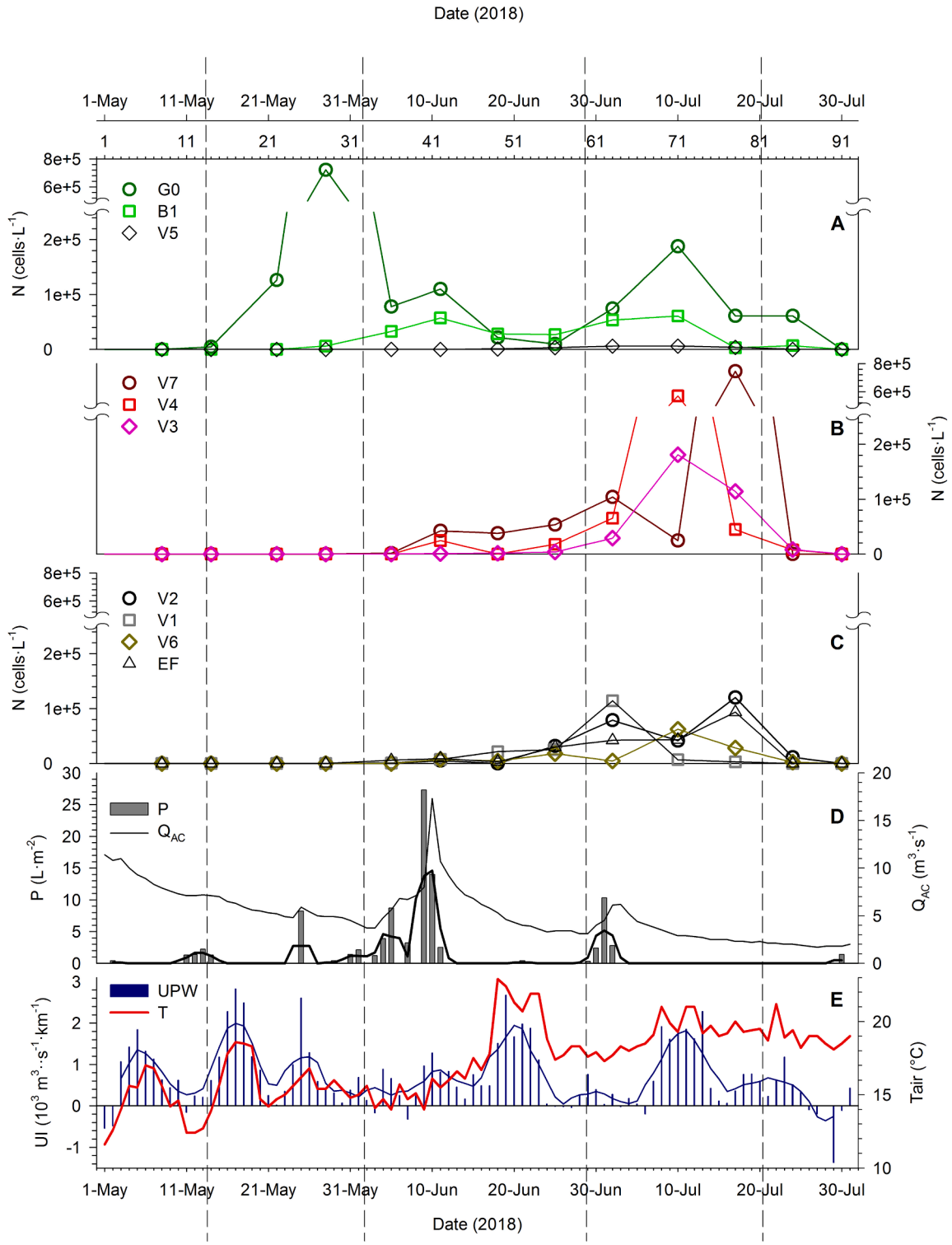

Fig. 3. Development of *A. minutum* bloom and associated meteorological conditions in 2018 (from 1st May to 30th July). Weekly time series of water column integrated (0–15 m) abundance (cells•L^{-1}) in: (A) Section from inner Baiona Bay to south mouth of Ría de Vigo (RV) (stations G0-B1-V5, Fig. 1C); (B) Southern margin of RV (towards the cul-de-sac along southern margin: V7-V4-V3) (RV); (C) Northern margin (from inner parts towards northern mouth of RV: V2-EF-V1-V6). Meteorological variability (daily values) of: (D) Precipitation (P, L$\cdot$m^{-2}; thin line) and river flow (aggregated from main rivers discharging in RV: Groba, Miñor, Lagares, Oitavén-Verdugo, Q_{AC}, m$^3\cdot$s^{-1}; bars -thick line, 3-day moving average); (E) Upwelling index (UI, 10^3 m$^3\cdot$s$^{-1}\cdot$km^{-1}, positive values indicate upwelling; bars -thin line, 3-day moving average) and air temperature (T, °C; daily average -thick line).

28th (Fig. 3A). During the following six weeks, *A. minutum* flourished in RV, progressing from the Baiona mouth (B1, ca. $6{\cdot}10^4$ cells·L^{-1} on June 11th) along the southern margin of RV towards the inner part (bloom transport and growth) (V7, ca. $5{\cdot}10^4$ cell·L^{-1} on 25th June; V4: ca. $7{\cdot}10^4$ cell·L^{-1} on 2nd July; and V3: $2{\cdot}10^5$ cell·L^{-1} on 9th July), and later on to its northern margin (bloom dispersion) (V2: 10^5 cell·L^{-1} on 16th July) (Fig. 3B-C). Bloom decayed on the 23rd July.

The proliferation of *A. minutum* in RP started three weeks later than in RV and ended one week later, following a comparable pattern (Supplementary Material S3A-B). It progressed outward from the inner part of Aldán, a small embayment similar to Baiona (bloom onset), and then spread towards the *cul-de-sac* of RP (bloom transport and growth), maintaining high concentrations for almost one month (bloom dispersion).

Red waters were continuously reported during July in both Rías, and the bloom caused prolonged harvesting closures due to the presence of paralytic shellfish toxins (PSTs) in mussels and infaunal molluscs. The sequence of closures followed the spatio-temporal dynamics of the bloom (INTECMAR weekly reports). Samples taken in the red tide contained 9.4–48.1·10^6 cells·L^{-1} on June 28th in Samil. The highest densities (166·10^6 cells·L^{-1}) were observed on July 9th in the Vigo marina, which concentrated the brown patches of *A. minutum*. Examination of the tidal cycle during several dates (9th, 12nd and July 20th) evidenced that surface patches of red waters were trapped into the dockyards during high tide, washing away at low tide (July 12nd, direct observation). These patches were usually concentrated in the upper 1–2 m layer and a sharp boundary between brown turbid and green clearer waters beneath the bloom was observed (see section 3.2.1. and Supplementary Material Video-File VF1).

3.1.3. Post 2018 bloom: distribution of resting cysts

Two types of cysts were observed in water samples collected in the red tide (Samil and Vigo marina sites): pellicle (thin-walled cysts) and resting cysts (thick-walled cysts). These two types matched descriptions of *A. minutum* cysts (Bravo et al. 2010b). The morphology of the cysts in the sediment during the survey carried out in March 2019 corresponded to those of resting cysts with an apparent cell wall. Results from the 13 sampling sites were pooled out as replicates representing 5 locations (Fig. 4; Table 1). Their concentrations in the first centimetre of the sediment showed high variability among stations (Fig. 4). The highest concentrations were detected in the sediment of Vigo marina with mean and maximum values of 2.7·10^3 cysts·cm^{-3} and 6.4·10^3 cysts·cm^{-3} of sediment, respectively. In the remaining stations, the highest mean and maximum values were observed in Baiona Bay close to the Miño estuary, where concentrations reached up 2.7·10^2 cysts·cm^{-3}.

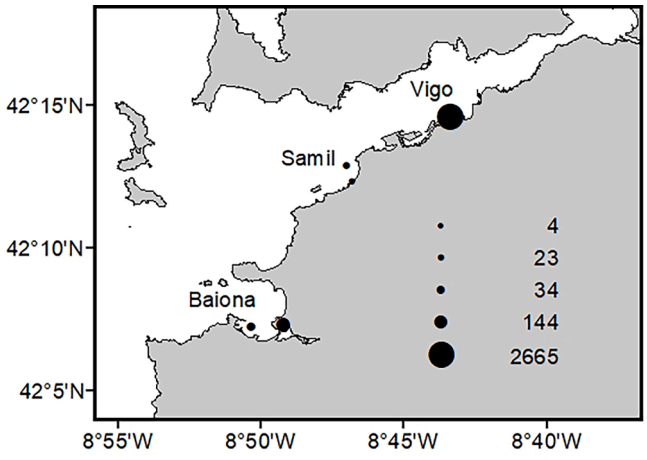

Fig. 4. *A. minutum* cysts distribution in the sediment of Ría de Vigo (average of the first cm of sediment, expressed as cysts·cm^3 of wet sediment) in March 2018.

3.2. Community assembly

3.2.1. HPLC pigment analyses

From HPLC analyses, highest Chl-*a* values in field samples from the red tide were recorded in semi-enclosed areas in the Vigo marina (221–692 μg Chl *a*·L^{-1}), the maximum being detected in the inshore pier (sampling point 4, Fig. 1) on July 15th. A high-resolution vertical profile in the upper 135 cm of the water column (July 18th, Vigo marina, sampling station 2) showed a steep decrease in *A. minutum* abundance below 0.4 m, although this patch was on the lowest range of densities observed in coloured waters (maximum of ~40 μg Chl *a*·L^{-1}, Fig. 5A). The overwhelming dominance of dinoflagellates (namely *A. minutum*, see 3.2.2.) in the field sample was evidenced from the parallel patterns of chlorophyll (Chl *a*) and Peridinin (Peri), an exclusive marker carotenoid for dinoflagellates (Rodríguez et al. 2020), together with the minor contribution of marker pigments for other algal groups. This is exemplified by two pigment chromatograms selected from that vertical profile (Fig. 5A). In the upper sample (marked with B in Fig. 5A) the chromatographic profile (Fig. 5B), nearly matched the composition of a Peri-containing dinoflagellate like *A. minutum*. In turn, a deeper sample (marked with C in Fig. 5A) showed a chromatogram (Fig. 5C) with increased proportions of other pigments such as the carotenoid fucoxanthin and chlorophyll c_1 (Fuco and Chl c_1, markers for diatoms and other chromophyte algae).

3.2.2. Microscopy and metabarcoding

Light microscope observations showed the overwhelming dominance of *A. minutum* in the bloom. The identity of the dominant species was unambiguously confirmed by epifluorescence examination of field samples and additional molecular characterization by sequencing the ITS rDNA marker of strain S1 from Samil. Light microscope observation also revealed that the dominant species was accompanied by minor amounts of other dinoflagellate genera (mainly *Heterocapsa*, *Prorocentrum* and *Scrippsiella*).

Community composition during the bloom was studied in detail using metabarcoding (V4 region of the 18S rRNA). *Alexandrium* sp. was the dominant species, accounting 70–95% of the reads (Fig. 6A, Table S1). The dominance of *Alexandrium* sp. was considerably higher in samples collected in the Vigo marina (sampling site 7, Fig. 1B; AL2-4, 86–95%) than in the sample collected outside the pier (AL1, 70%). Among the 147 ASVs identified, 22 corresponded to *Alexandrium* sp. of which only one was very abundant (68.9–93.6% of reads) while the others were scarce (<1% of reads).

In addition to *Alexandrium* sp., the 18S rRNA metabarcoding analyses detected other Dinophyceae (43 ASVs), diatoms (28 ASVs), the parasite *Parvilucifera* (Perkinsea, 3 ASVs), ciliates (13 ASVs), marine alveolates (MALV, 6 ASVs), metazoa (15 ASVs), and other groups with minor abundances represented by one to three ASVs (Table S1). The relative abundance of groups accompanying *Alexandrium* sp. was higher in the sample collected outside the pier (AL1) than in the three samples collected in the marina (Fig. 6B). There, other dinoflagellates, diatoms and marine alveolates were the most abundant groups, accounting up to 12, 6 and 13% of reads respectively. Only 13 ASVs were shared among the four analysed samples, while 92 ASVs were exclusively found in one of the samples (Fig. 6C), suggesting a relevant variability at small spatial and temporal scales in the assemblage that accompany *Alexandrium* sp.

A more detailed analysis of the taxonomic groups of the Dinophyceae in the bloom of *Alexandrium* sp. revealed a similar composition of the assemblage at the order level, but the relative abundance of these groups varied among samples (Fig. Supplementary Material S4). Metabarcoding analyses confirmed microscopic observations of the genera *Heterocapsa*, *Scrippsiella* and *Prorocentrum*, but also revealed a much more diverse assemblage, with ASVs assigned to other 17 genera.

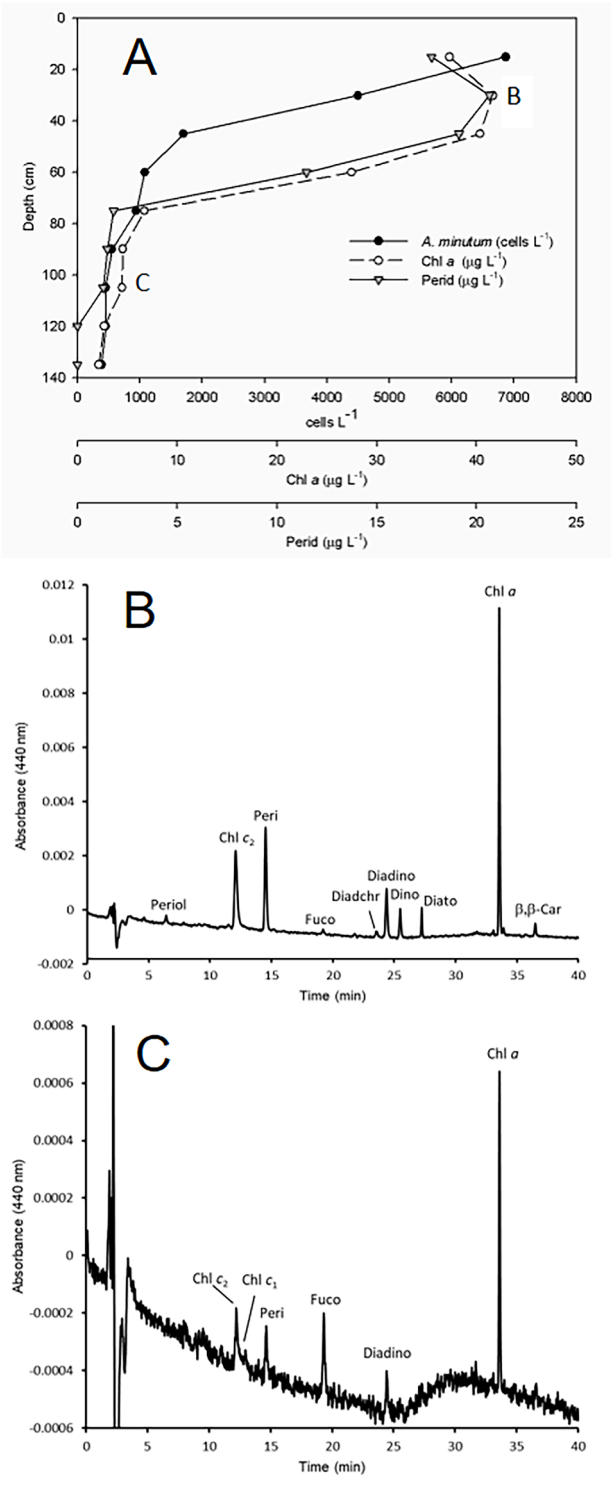

Fig. 5. HPLC pigment analysis of red tide waters. (A) Vertical profile of *Alexandrium minutum* (cells·L^{-1}) at sampling station 2 (Vigo marina, July 18th), with associated HPLC pigment data for Chl *a* and Peridinin (µg·L^{-1}). Samples belonging to chromatograms in pannels B and C are indicated in the vertical profile. (B) Chromatogram of a sample at 30 cm depth from station 2. (C) Chromatogram of a sample at 105 cm depth from station 2. Pigment abbreviations: Peridinol (Periol), Chlorophyll c_2 (Chl c_2), Chlorophyll c_1 (Chl c_1), Peridinin (Peri), Fucoxanthin (Fuco), Diadinochrome (Diadchr), Diadinoxanthin (Diadino), Dinoxanthin (Dino), Diatoxanthin (Diato), β,β-carotene (β,β-Car).

3.3. Particle tracking model

3.3.1. Meteorological drivers: variability during the 2018 bloom

Weather conditions during the 2018 bloom differed from climatic averages due to high precipitation/runoff recorded in June (108% higher rainfall than the monthly average for the reference period 1981–2010; Meteogalicia, 2018), as well as high upwelling intensity in May and, to a lesser extent, in June (426 and 184% higher than monthly averages of the upwelling index for these months for the reference period 1970–2018; historical FNMOC data series).

Time series of daily averaged precipitation and runoff (Fig. 3D) show that higher values were recorded in the first half of June due to the passage of a weather frontal system. Maximum aggregated flow (ca. 16 $m^3 \cdot s^{-1}$) was recorded on June 10th, one day lagged to the peak of precipitation (27 $L \cdot m^{-2}$). Concurrently, moderate-high (8–15 $m \cdot s^{-1}$) westerly winds and upwelling relaxation predominated during this period (Fig. 3E), which was coincident with the spread of *A. minutum* out of Baiona Bay towards the inner part of RV along its southern margin (Fig. 3A-B). A similar scenario occurred at the end of June, associated to the passage of another front and the associated precipitations / runoff, moderate-high westerlies and upwelling relaxation. This event is concurrent with the extension of the bloom from the already *A. minutum* populated southern margin of RV to the rest of the embayment (Fig. 3B-C).

3.3.2. Model simulations

Results from the particle tracking model reproduce the observed bloom dynamics in RV (Figs. 7 and 8). Model simulations show that for most of the studied period, meteorological conditions provoke the confinement of the passive tracers within the upwelling shadow zone shaped by Baiona Bay (modelling case 1, Fig. 7). This situation changed in June 8th, when strong south, south-westerly winds and associated precipitation / runoff force particles outside the bay, and their spread along the southern margin of RV (Supplementary Material S5A-B). Particles released in Baiona Bay after this date remained inside the embayment all over the period of bloom development, as was tested in the simulations (not shown).

Results from modelling case 2 (Fig. 7) simulate the behaviour of particles released from two boxes (enclosing Samil - Vigo and Chapela) during June and July, when these areas of the southern margin were already populated by *A. minutum*. The series of maps in Fig. 8 describe the most typical situations that appear over the entire period. The two most frequent situations are the one corresponding to the simulation on the 16th June (Fig. 8A), in which the particles remain stuck to the south shoreline under strong northerly, upwelling favourable winds over the shelf and weak winds inside RV (Supplementary Material S6A-B), or have an oscillatory movement whose final result is their retention inside RV under moderate southerly, downwelling favourable winds over the shelf and weak winds inside RV (simulation on the 3rd July, Fig. 8C). Among these alternating situations, under variable and weak northerly winds, such as those experienced from the 19th to 23rd June, the particles leave RV through the northern mouth. During the entire period of the simulation, this situation only occurs during this period of time (simulation corresponding to the 21st June, Fig. 8B). Another situation occurred under strong northerly winds over the shelf and inside the Ría (simulation on the 7th July, Fig. 8D), which cause periods in which the particles approach the south shoreline, and tend to be exported outside RV across the southern mouth.

4. Discussion

The present study accounts for an exceptional red tide of *A. minutum* in NW Spain that caused prolonged harvesting closures due to the occurrence of PSTs in shellfish (Ben-Gigirey et al. 2020). Its occurrence and the environmental conditions favouring the development of *A. minutum* in the area have been previously examined (Bravo et al.

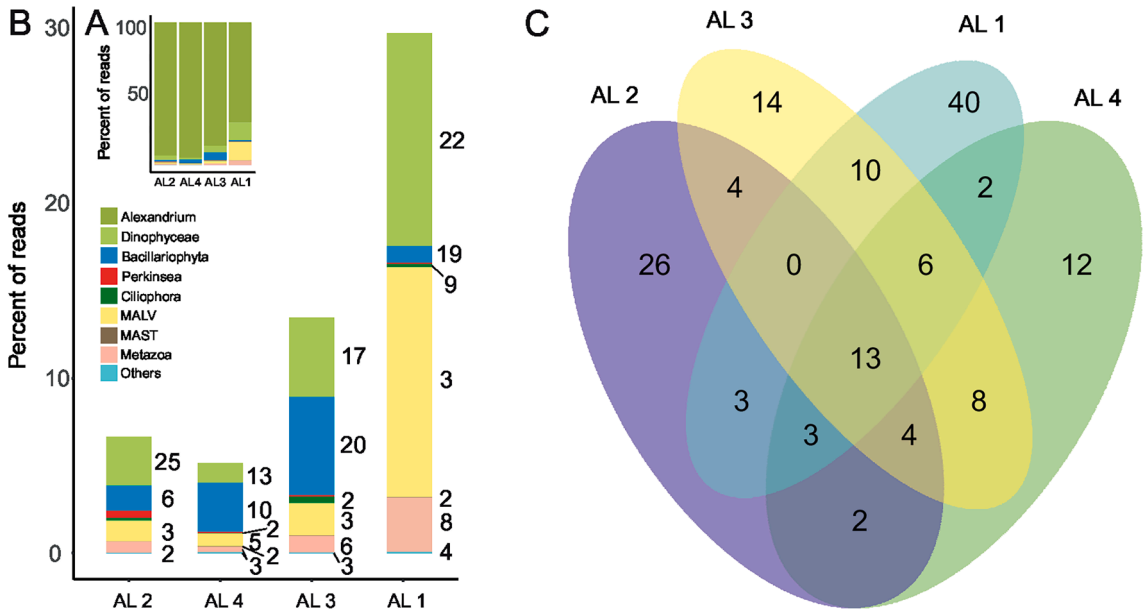

Fig. 6. Relative abundance of metabarcoding reads of the major taxonomic groups in which ASVs were classified (Table S1) including (A) or excluding (B) *Alexandrium minutum* and (C) Venn diagrams showing the overlap between the ASVs identified in the metabarcoding analyses in the four analysed samples. In A and B, numbers indicate the diversity of ASVs for each group (only shown if > 1). Sample codes are as follows: AL1 (sampling site 7, but open waters instead of inside the Vigo marina; July 20), AL2 and AL4 (sampling site 7, July 10 and 12), AL3 (sampling site 4, July 12).

2010a). However, unlike former events in the area, the spatial extension and attained cell concentrations during the 2018 bloom and, later on, of resting cysts in the sediment, showed its consequences in the following years, with the recurrence of *A. minutum* in the Rías Baixas in 2019 and 2020. We hypothesize here that environmental conditions associated to global climate change trends promoted this unusual succession of events.

4.1. Bloom dynamics of Alexandrium minutum and red tides in NW Spain

The dynamics of blooms caused by different species of *Alexandrium* are not entirely understood due to the contrasting environmental conditions driving their occurrence (Anderson et al., 2012). In the particular case of *A. minutum*, its blooms have been related to water stability, salinity stratification and local nutrient-rich freshwater inputs, particularly in estuaries, protected harbours and lagoons (Giacobbe et al., 1996; Maguer et al., 2004; Vila and Masó, 2005; Bravo et al., 2008, 2010a; Santos et al., 2014; Guallar et al., 2017; Gladan et al., 2020). So far, in the Iberian Peninsula, the most intensive blooms of this species (up to $47{\cdot}10^6$ cells·L^{-1}) have been reported in the Mediterranean Sea harbours (Garcés et al., 2004; Vila and Masó, 2005), similarly to the bloom in Vigo in 2018 (up to $166{\cdot}10^6$ cells·L^{-1}).

In the northeast Atlantic Ocean, *A. minutum* blooms are regularly observed in the French coastline between Charente and Brittany departments associated with estuaries (Guallar et al., 2017). Giacobbe et al. (1996) also showed the development of *A. minutum* populations during springtime in a brackish Mediterranean lagoon after enhanced rainfall and freshwater runoff, which reinforced water column (haline) stratification. Same conditions were also observed prior to the *A. minutum* bloom in a coastal lagoon in S. Jorge Island (Azores) (Santos et al., 2014) and before the *A. minutum* bloom in Ría de Ares in May 1984 (Blanco et al., 1985). The latter followed heavy rains (275% higher than the historical monthly average) and maximum densities (10^7 cells L^{-1}) were recorded in the halocline established by the riverine inputs in the inner part of that Ría (at salinities of 22–27). The bloom disappeared once southerly winds eroded the stratification in July. Again, the sequence of heavy rains and stratification was associated to a bloom of *A. minutum* in the Miño estuary in 2006 (Baiona Bay), though cell concentrations were lower, reached a peak value of ca. 10^6 cells·L^{-1} (Bravo et al., 2010a).

To our knowledge, there are no historical records of *A. minutum* red tides in the Rías Baixas. The former reports of massive red tides in this area were those aforementioned in 1916–17 (de Buen, 1916, Sobrino, 1918) due to *Lingulodinium polyedra* and later in the 50′s (Margalef, 1956). The accounts from these authors suggest that red tides were impressive and common, to such extent that the accumulation and decomposition of organic matter after their decline throughout time was interpreted as the cause of collapse of a newly built dockyard in the Vigo marina in 1915 (Memoria sobre el estado de las obras del Puerto de Vigo en 31 de diciembre de 1926, 1927, Bruna, 2017).

After that period, the lack of historical reports until the 70′s reflects the absence of surveys. Later on, despite the continuous research efforts and the beginning of the Galician HAB monitoring programme since the 80′s, the occurrence of red tides due to toxic dinoflagellates has been anecdotal. The few occasions when, to our knowledge, discoloured waters have been noticed correspond to PSP events in 1976 and 1986 by *Gymnodinium catenatum*. Only the ciliate *Mesodinium rubrum* and the dinoflagellate *Noctiluca scintillans*, two common non-toxic red tide producers in the Rías Baixas, have been responsible of discoloured waters over large areas, mostly localized in a single Ría. These reasons explain the great attention that deserved this exceptional toxic bloom in 2018 (Ben-Gigirey et al., 2020), from the local and national media [e.g. Faro de Vigo (17-VII-2018): https://www.farodevigo.es/gran-vigo/2018/07/17/marea-roja-expande-darsenas-urbanas/1929438.html; Antena 3 (22-VII-2018): https://www.antena3.com/noticias/sociedad/la-marea-roja_201807225b54e27e0cf229e4f541dd17.html].

4.2. The extreme 2018 red tide: relationship with environmental factors

The year 2018 was singular for several reasons, both before and during the *A. minutum* red tide. First to mention the weather conditions, with heavy precipitations, late in the season and higher than the monthly historical average, followed by a sudden rise of air temperature and daily irradiance two weeks before the bloom. Overall, our analysis suggests that the stabilisation in the upper layer in Ría de Vigo, triggered by the combination of intense continental runoff and increased

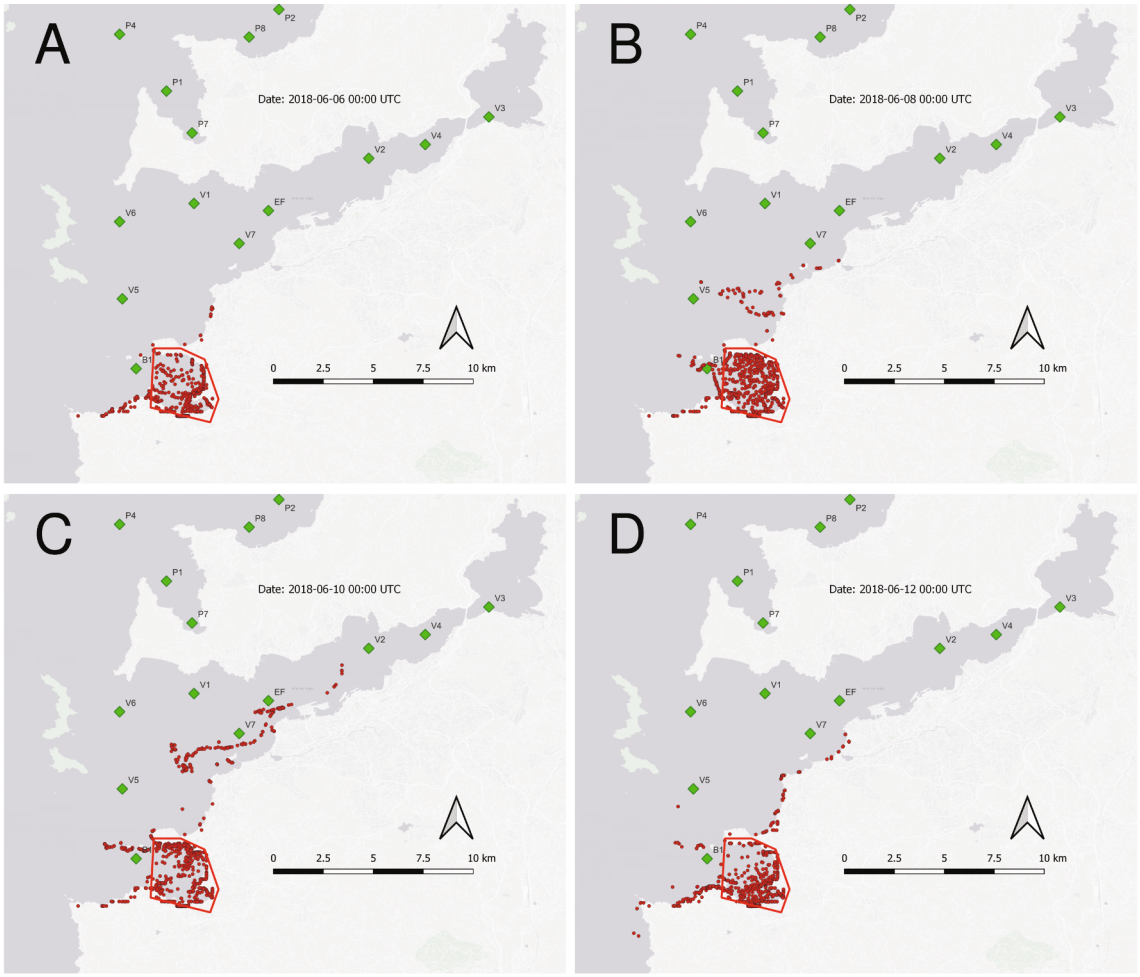

Fig. 7. Particle tracking model1: Case 1. Simulation of bloom onset and retention in Baiona Bay (6th June, 7A), following dispersion from there to Ría de Vigo favoured by the passage of a frontal system and the concomitant short-term change (from 8th to 12th June, 7B-D) in local meteorological and hydrographic conditions (Fig. 3D-E and Suppl. Mat. S5A-B). Particle emission box (red line contour) corresponds to Baiona Bay. (For interpretation of the references to colour in this figure legend, the reader is referred to the web version of this article.)

insolation was a first requisite for the onset of favourable conditions for the development of *A. minutum* populations that seeded the red tide event. In addition, upwelling favourable conditions lifted up the pycnocline and enhanced the temperature gradient, confining the populations to a well-lit stable layer (~upper 10 m depth) during an extended period, from the second half of June through July (e.g. Suppl. Mat. S3C). The effect of upwelling dynamics on the vertical structure of the water column can be tracked on temperature profiles acquired at station EF on RV (Suppl. Mat. S7), which illustrate the ascent / descent of the thermocline and increment / decrement of stratification during spin-up / spin-down phases of upwelling cycles (e.g. temperature profiles on the 10 and 17 July during, respectively, spin-up and spin-down phases of upwelling -Fig. 3E) [Additional hydrographic profiles can be consulted using the CTD visor in the INTECMAR webpage: http://www.intecmar.gal/Ctd/Default.aspx]. These conditions resemble the 1984 bloom in Ría de Ares, which was associated with northern winds and stratified waters (Blanco et al., 1985).

In Ría de Vigo in 2018, *A. minutum* was first detected in significant numbers in Baiona (Stns. B1 and G0 on May 28th), and afterwards spread into that Ría, initially along the southern margin and later on along the northern one. A similar pattern was observed in Ría de Pontevedra, where noticeable abundances of *A. minutum* were first detected in Aldán (station P1 on June 25th) before spreading inward along the southern and northern margins. Both Baiona and Aldán have in common that they are small, relatively shallow estuaries with low river flow at their head, northward oriented and lying in the southern margin, close to the mouth of their respective Rías (Fig. 1) (Alejo et al., 1999; Lourido et al., 2010). This physiographic configuration favours the development of relatively intense water column stratification, both of haline and thermal origin, and shape an upwelling shadow zone (Supplementary Material S5A-B and S6A-B) where the influence of coastal upwelling and the associated off-shoreward wash-out diminishes. These stratification-enhanced, upwelling shadow zones function as retention areas for plankton (e.g. Morgan and Fisher, 2010; Ryan et al., 2014), providing a favourable niche for the development of *A. minutum* as the historical records of occurrence of this species (1998–2020) suggest, although in relatively low abundances, in the aforesaid small inner estuaries during spring-summer.

We hypothesize that the 2018 bloom developed initially in those areas, attaining high abundances in the upper surface layer (<5m) under favourable stratified and nutrient-rich environment linked to relatively intense freshwater discharges. Intense rains / river discharges and westerly winds in the first weeks of June would lead to the bloom spreading into the Rías. The results from the particle tracking model support this hypothesis. Upwelling conditions were strong from mid-June and July, but not enough to erode the strongly stratified less saline warm upper layer where the bloom evolved (Suppl. Mat. S7). The Vigo marina could have acted as a *cul-de-sac* where these surface layers entered during the high tide, raising steeply their abundance in comparison with surface waters outside the pier in Ría de Vigo. A similar

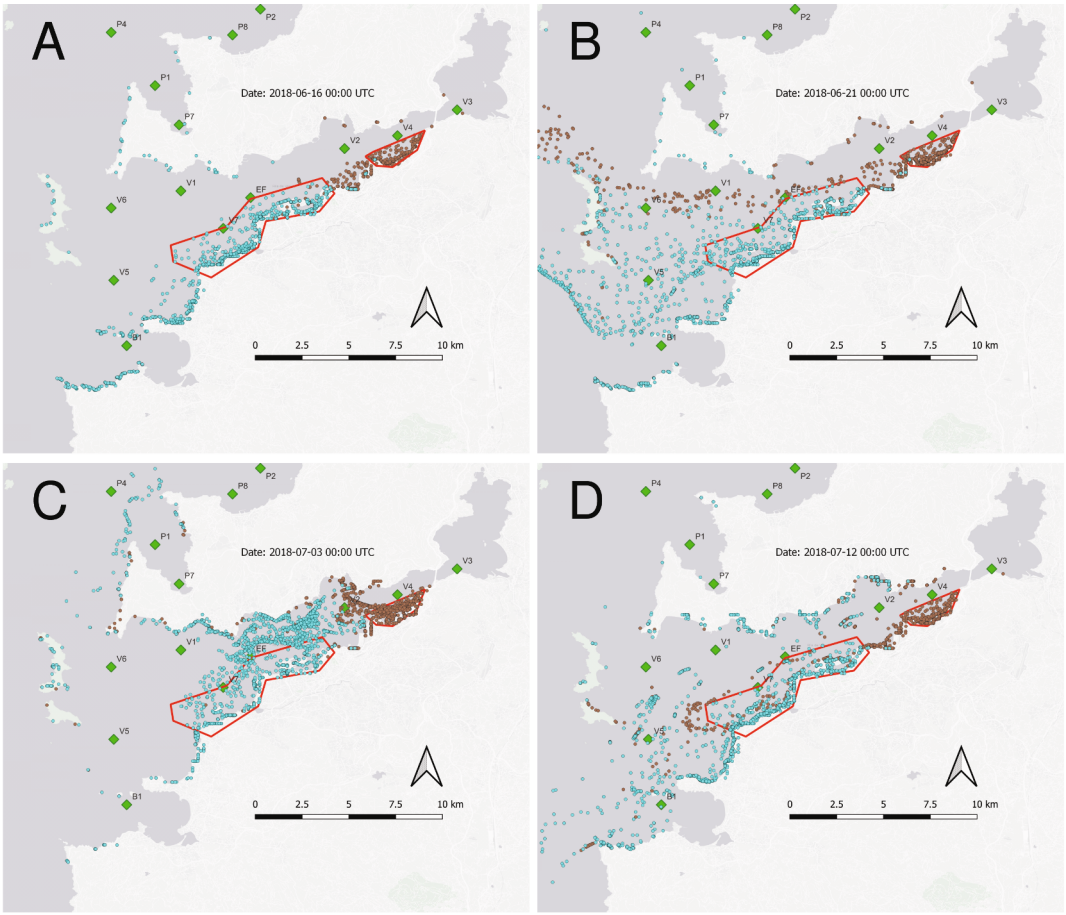

Fig. 8. Particle tracking model: Case 2. Simulation of the spread of the bloom from the already populated southern margin of Ría de Vigo using two particle emission boxes (red line contours), one southern embracing Samil beach and the Port of Vigo, the northern corresponding to the cove of Chapela. Blue and brown dots correspond to particles from Samil and Vigo harbour emission box and Chapela bay emission box, respectively. The simulation period runs from 6th June to 23rd July (8A-D). Snapshots of model runs corresponding to 16th and 21st June and 7th and 12th July (Suppl. Mat. S6A-B for wind and surface current fields for the selected model run snapshots). (For interpretation of the references to colour in this figure legend, the reader is referred to the web version of this article.)

situation could have occurred in the southern and northern margins of the Ría de Pontevedra. This would also explain the exceedingly high Chl *a* level registered in the Vigo marina, and the dominance of a "pure" dinoflagellate assemblage with a field pigment signature overwhelmed by peridinin. In that sense, it must be noted that pigment composition in the Galician Rías is often dominated by nano-microplankton fucoxanthin-containing groups, in agreement with the prominent position of diatoms in this highly productive area (Rodríguez et al., 2003; Figueiras et al., 2020).

Finally, it should not be dismissed the potential contribution of the intense wildfires registered in the Vigo area in October 2017 to fuel plankton growth in 2018. Unfortunately, there is a lack of studies of wildfire impacts in marine ecosystems in comparison with those in freshwater habitats, especially on streams (Silins et al., 2014; Bixby et al., 2015). Increased soil erosion and sediment loss after wildfires can greatly disturb aquatic ecosystems, for instance through an excess of nutrients leading to algal blooms. However, the effects on algal populations can be also negative or neutral (Klose et al., 2015) due to differences among terrestrial habitats, vegetation, and other biotic and abiotic factors (such as light and temperature). Notwithstanding, the fertilization of phytoplankton by ash and/or continental runoff after wildfires has been scarcely studied. Only recently, wildfire and volcanic ashes have been identified as causative agents of phytoplankton blooms in Indonesian coastal waters (Abram et al., 2003), the Northeastern Pacific (Langmann et al., 2010) and the Southern Ocean (Tang et al., 2021). The putative role of wildfires to promote plankton growth in coastal regions, particularly in confined environments with restricted circulation that can act as seed beds, merits further research efforts, as preliminary evidences on their positive effects in natural phytoplankton communities are being gathered (Ladd et al., 2020).

Fertilization due to upwelled cold waters in the Rías Baixas could by itself (plus other factors as mentioned above) supply the amount of nutrients needed to fuel the growth of *A. minutum* populations, until a combination of dispersion, nutrient exhaustion or other biological factors such as grazing or encystment led to the gradual decline of cell numbers towards the end of July. In that sense, resting cyst formation was not significant in the two field samples incubated in the laboratory, and therefore, these results were not included in the manuscript. But the confinement of the population allowed to detect *Parvilucifera* infections (Supplementary Material Video File VF2), despite the fact that these incubations did not follow any specific protocol to detect the parasite. *A. minutum* infections by *Parvilucifera* sp. were qualitatively reported due to their interest, given the potential role of parasites to explain bloom collapse. Actually, infections by *Parvilucifera* sp. parasitoids were generalized after ~72 h of incubation.

4.3. Cyst based seeding strategy and recurrence

Resting cysts of *A. minutum* have been suggested to provide the inoculum for its blooms, supplying the essential resource for its characteristic seasonality. This process has been described in areas with high hydrodynamics such as estuaries subjected to tidal streams (Bravo et al.,

2010b; Giacobbe et al., 1996) but also in calmer semi-enclosed waters like harbours (Garcés et al., 2004; Estrada et al., 2010). Baiona Bay gathers suitable characteristics for *A. minutum* bloom development. There, resting cyst formation has been described during the terminal phase of a bloom associated with a strong stratification in the Miño river estuary that empties into Baiona Bay (Bravo et al., 2010b). These cysts probably provide the inoculum of the proliferations that recurrently occur in this area and could have been the origin of the bloom in 2018. The model herein included confirms the feasibility of such hypothesis: the inoculum population could be established in Baiona and it could spread afterwards into Ría de Vigo.

The present work also describes the accumulation of cysts in the Vigo marina. This area, along with other harbours in Ría de Vigo, provided shelter for the 2018 bloom. The cysts detected several months after the bloom evidence Vigo marina as an important cyst reservoir in comparison to other less protected sampling areas (though our results probably show only a small part of the actual cyst reservoir). Germination of these cysts likely led to the extended proliferations detected in 2019 and 2020, and it is possible that the same might occur in the near future.

The hypothesis that discrete seedbeds of resting cysts provide the inoculum for recurrent *Alexandrium* blooms has been frequently suggested in the literature (Anderson, 1998; Stock et al., 2005; Lau et al., 2017; Lewis et al., 2018). Regarding *A. minutum*, life cycle alternations between resting cysts and vegetative cells were described in the harbours of the Catalonian coast, providing an efficient strategy for the recurrence of intense blooms in that area (Anglès et al., 2012).

4.4. Is there a link between the extreme 2018 bloom and regional climate trends?

It is tempting to tag exceptional events like the 2018 bloom as an example of HABs associated with global change. A special issue on the state of the climate in NW Iberia (Gimeno et al., 2011) summarized the tendencies and expected evolution in land and sea. Within that issue, Gómez-Gesteira et al. (2011) indicated a significant increase between 1974 and 2007 in air and sea temperatures of 0.5 °C and 0.24 °C per decade, respectively. Overall, precipitations showed ample seasonal variability but no significant long-term trends (1930–2006; Vicente-Serrano et al., 2011).

In Vigo, between May and July, precipitations have declined particularly in May (<40% in 2011–2020 relative to 1961–1970), but no trends emerge in the following months (ECAD; Vigo-Peinador station). A significant decadal air warming of 0.42 °C and 0.30 °C was detected between May and June-July, respectively. In June 2018 a strong positive anomaly in precipitations (>200% than the average for 2011–2020) was accompanied by high air temperatures (but within the range in the last decade). Unfortunately, available records of sea surface temperatures in the Rías Baixas only cover a short period 2006–2019, and potential shifts in some relevant stations for this study were not detected: G0 (Baiona), V5 (Vigo) and P7 (Pontevedra).

Positive feedback with climate trends could be argued if favourable conditions for the development of *A. minutum* blooms, i.e. heavy rains in late spring/summer, followed by high temperatures and feeble winds fostering haline / thermal stratification in the upper layers, became more frequent. In this sense, the reduction in the upwelling period and its weakening in NW Iberia, that especially affected the Rías Baixas (Álvarez-Salgado et al., 2008), is projected to follow up in this century due to sea surface warming (Sousa et al., 2020). Overall, this situation could likely provide a favourable scenario for HAB proliferations in the near future, including those of *A. minutum* in the Rías Baixas.

5. Conclusions

A combination of unusual weather conditions during May-July (wind regime, precipitations and continental runoff, as well as temperature) explained the onset and development of a massive red tide of *A. minutum* in surface waters in Ría de Vigo and Pontevedra without precedent in the region. Assuming that stable, stratified environments, such as those shaped in upwelling shadow zones, favour retention and/or *in situ* growth of potentially harmful dinoflagellate populations, it is feasible that the effect of global warming together with other factors (e.g. cyst seeding) could turn these proliferations into a new normality in these areas. The present study contributes to the general understanding of the environmental factors triggering *A. minutum* blooms, enlarging our body of knowledge about the proliferations of this global HAB species. Furthermore, considering the application of HAB species as indicators of ecosystem status, for instances in the frame of recent EU environmental policies such as the Marine Strategy Framework Directive, our findings are of interest not only at local or regional scales but also for other geographical areas sharing similar characteristics. Finally, an increase in both the frequency and intensity of *A. minutum* proliferations in the area, as well as its regional expansion, could take place in the coming years due to both the consequences derived from the 2018 bloom (the formation of resting cyst beads) and the probably recurrence of the climate scenario that fostered this unusual intense event.

CRediT authorship contribution statement

E. Nogueira: Conceptualization, Data curation, Formal analysis, Software, Supervision, Validation, Visualization, Writing – original draft, Writing – review & editing. **I. Bravo:** Conceptualization, Formal analysis, Funding acquisition, Investigation, Methodology, Project administration, Resources, Supervision, Validation, Writing – original draft, Writing – review & editing. **P. Montero:** Formal analysis, Software, Validation, Visualization, Writing – original draft, Writing – review & editing. **P. Díaz-Tapia:** Formal analysis, Methodology, Resources, Software, Supervision, Validation, Visualization, Writing – original draft, Writing – review & editing. **S. Calvo:** Data curation, Methodology, Resources, Supervision, Validation, Writing – review & editing. **B. Ben-Gigirey:** Methodology, Validation, Writing – original draft, Writing – review & editing. **R.I. Figueroa:** Funding acquisition, Investigation, Methodology, Project administration, Resources, Writing – original draft, Writing – review & editing. **J.L. Garrido:** Formal analysis, Methodology, Visualization, Writing – original draft, Writing – review & editing. **I. Ramilo:** Methodology, Software, Visualization. **N. Lluch:** Methodology. **A.E. Rossignoli:** Methodology, Validation, Writing – original draft, Writing – review & editing. **P. Riobó:** Methodology, Validation, Writing – original draft. **F. Rodríguez:** Conceptualization, Formal analysis, Investigation, Methodology, Supervision, Validation, Writing – original draft, Writing – review & editing.

Declaration of Competing Interest

The authors declare that they have no known competing financial interests or personal relationships that could have appeared to influence the work reported in this paper.

Acknowledgments

We acknowledge Y. Pazos, F. Amoedo, A. Bértolo, P. García, I. Lemos, M. Pérez and S. Roura from “Unidad de Oceanografía y Fitoplancton” (INTECMAR), for weekly cell count data obtained on course of the Galician monitoring programme. We wish also to thank several public institutions which collect and offer online environmental data included in this study: hydrographical and meteorological variables (INTECMAR and MeteoGalicia) and rivers flow data supplied by Augas de Galicia. We acknowledge also P. Loures and P. Rial for technical assistance with laboratory cultures, and C. Carballeira for technical assistance with HPLC pigment analyses. We greatly appreciate also the collaboration of J. Hernández-Urcera and M. Garci (IIM-CSIC) for scuba dive samples in the Vigo marina, and M. García-Portela, L. Feáns, and M. Pazos for collaboration during red tide sampling. We thank Marta M. Varela for

her helpful comments on the manuscript. High-performance computing analysis was run by means of the remote supercomputing resources of the Centro de Supercomputación de Galicia (CESGA). This work was funded by the Spanish national project DIANAS (CTM2017-86066-R, MICINN) and CCVIEO (Instituto Español de Oceanografía). PD-T was supported by the Xunta de Galicia program "Talento Senior" (N° contract 03 IN858A 2019 1630129) with additional funds of the Axencia Galega de Innovacion (agreement GAIN-IEO). This is a contribution of Unidad Asociada IEO-CSIC Microalgas Nocivas.

Appendix A. Supplementary data

Supplementary data to this article can be found online at https://doi.org/10.1016/j.ecolind.2022.108790.

References

Abram, N.J., Gagan, M.K., McCulloch, M.T., Chappell, J., Hantoro, W.S., 2003. Coral reef death during the 1997 Indian Ocean dipole linked to Indonesian wildfires. Science 301, 952–955. https://doi.org/10.1126/science.1083841.

Alejo, I., Austin, W.E.N., Francés, G., Vilas, F., 1999. Preliminary investigations of the recent Foraminifera of Baiona Bay, N.W. Spain. J. Coast. Res. 15, 413–427.

Allen, C.M., 1982. Numerical simulation of contaminant dispersion in estuary flows. P. R. Soc. London A 381, 179–194. https://doi.org/10.1098/rspa.1982.0064.

Álvarez-Salgado, X.A., Labarta, U., Fernández-Reiriz, M.J., Figueiras, F.G., Rosón, G., Piedracoba, S., Filgueira, R., Cabanas, J.M., 2008. Renewal time and the impact of harmful algal blooms on the extensive mussel raft culture of the Iberian coastal upwelling system (SW Europe). Harmful Algae 7, 849–855. https://doi.org/10.1016/j.hal.2008.04.007.

Anderson, D.M., 1998. Physiology and bloom dynamics of toxic *Alexandrium* species, with emphasis on life cycle transitions. In: Anderson, D.M., Cembella, A.D., Hallegraeff, G.M. (Eds.), Physiological Ecology of Harmful Algal Blooms. Springer-Verlag, Berlin-Heidelberg, pp. 29–48.

Anderson, D.M., Alpermann, T.J., Cembella, A.D., Collos, Y., Masseret, E., Montresor, M., 2012. The globally distributed genus *Alexandrium*: Multifaceted roles in marine ecosystems and impacts on human health. Harmful Algae 14, 10–35. https://doi.org/10.1016/j.hal.2011.10.012.

Anderson, D.M., 2014. HABs in a changing world: a perspective on harmful algal blooms, their impacts, and research and management in a dynamic era of climactic and environmental change. Proc 15th Int Conf Harmful Algae, p 3-17.

Anglès, S., Garcés, E., Reñé, A., Sampedro, N., 2012. Life-cycle alternations in *Alexandrium minutum* natural populations from the NW Mediterranean Sea. Harmful Algae 16, 1–11. https://doi.org/10.1016/j.hal.2011.12.006.

Arístegui, J., Barton, E.D., Álvarez-Salgado, X.A., Miguel, A., Santos, P., Figueiras, F., Kifanid, S., Hernández- León, S., Mason, E., Machú, E., Demarcq, H., 2009. Sub-regional ecosystem variability in the Canary Current upwelling. Prog. Oceanogr. 83 (1–4), 33–48. https://doi.org/10.1016/j.pocean.2009.07.031.

Ben-Gigirey, B., Rossignoli, A.E., Riobó, P., Rodríguez, F., 2020. First report of paralytic shellfish toxins in marine invertebrates and fish in Spain. Toxins 12 (11), 723. https://doi.org/10.3390/toxins12110723.

Bixby, R.J., Cooper, S.D., Gresswell, R.E., Brown, L.E., Dahm, C.N., Dwire, K.A., 2015. Fire effects on aquatic ecosystems: an assessment of the current state of the science. Freshw. Sci. 34, 1340–1350. https://doi.org/10.1086/684073.

Blanco, J., Mariño, J., Campos , M.J., 1985. The first toxic bloom of *Gonyaulax tamarensis* detected in Spain. In: Anderson, D.M., White, A.W., Baden, D.G. (eds) Toxic dinoflagellates. Proc 3rd Int Conf Toxic Dinoflagellates, St. Andrews, New Brunswick, Canada. Elsevier Science Publishing Co. Inc., p 79-84.

Braunschweig, F., Leitão, P., Fernandes, L., Pina, P., Neves, R.J.J., 2004. The object-oriented design of the integrated water modelling system MOHID. Dev. Water Sci. 55, 1079–1090. https://doi.org/10.1016/S0167-5648(04)80126-6.

Bravo, I., Fraga, S., Figueroa, R.I., Pazos, Y., Massanet, A., Ramilo, I., 2010a. Bloom dynamics and life cycle strategies of two toxic dinoflagellates in a coastal upwelling system (NW Iberian Peninsula). Deep Sea Res. Part II Top. Stud. Oceanogr. 57, 222–234. doi: 10.1016/j.dsr2.2009.09.004.

Bravo, I., Garcés, E., Diogène, J., Fraga, S., Sampedro, N., Figueroa, R., 2006. Resting cysts of the toxigenic dinoflagellate genus *Alexandrium* in recent sediments from the Western Mediterranean Coast, including the first description of cysts of *A. kutnerae* and *A. peruvianum*. Eur. J. Phycol. 41, 293–302. https://doi.org/10.1080/09670260600810360.

Bravo, I., Vila, M., Masó, M., Figueroa, R.I., Ramilo, I., 2008. *Alexandrium catenella* and *Alexandrium minutum* blooms in the Mediterranean Sea: Toward the identification of ecological niches. Harful Algae 7, 515–522. https://doi.org/10.1016/j.hal.2007.11.005.

Bravo, I., Figueroa, R.I., Garcés, E., Fraga, S., Massanet, A., 2010b. The intricacies of dinoflagellate pellicle cysts: The example of *Alexandrium minutum* cysts from a bloom-recurrent area (Bay of Baiona, NW Spain). Deep Sea Res. Part II Top. Stud. Oceanogr. 57, 166–174. https://doi.org/10.1016/j.dsr2.2009.09.003.

Bruna, B., 2017. Efemérides del Puerto de Vigo. Autoridad Portuaria de Vigo, archivo general del Puerto de Vigo 49, p 16.

Callahan, B.J., McMurdie, P.J., Rosen, M.J., Han, A.W., Johnson, A.J.A., Holmes, S.P., 2016. DADA2: High-resolution sample inference from Illumina amplicon data. Nat. Methods 13, 581–583. https://doi.org/10.1038/nmeth.3869.

Carracedo, P., Torres-López, S., Barreiro, M., Montero, P., Balseiro, C.F., Penabad, E., Leitão, P., Pérez-Muñuzuri, V., 2006. Improvement of pollutant drift forecast system applied to the Prestige oil spills in Galicia Coast (NW of Spain): development of an operational system. Mar. Pollut. Bull. 53, 350–360. https://doi.org/10.1016/j.marpolbul.2005.11.014.

De Buen, O., 1916. Trabajos españoles de oceanografía: campaña del Hernán Cortés este verano. Boletín de Pescas 3, 1–9.

Declerck, A., Delpey, M., Rubio, A., Ferrer, L., Basurko, O.C., Mader, J., Louzao, M., 2019. Transport of floating marine litter in the coastal area of the south-eastern Bay of Biscay: A Lagrangian approach using modelling and observations. J. Oper. Oceanogr. 12, S111–S125. https://doi.org/10.1080/1755876X.2019.1611708.

Díaz, P., Ruiz-Villareal, M., Pazos, Y., Moita, T., Reguera, B., 2016. Climate variability and *Dinophysis acuta* blooms in an upwelling system. Harmful Algae 53, 145–159. https://doi.org/10.1016/j.hal.2015.11.007.

Estrada, M., Solé, J., Anglès, S., Garcés, E., 2010. The role of resting cysts in *Alexandrium minutum* population dynamics. Deep Sea Res. Part II Top. Stud. Oceanogr. 57, 308–321. https://doi.org/10.1016/j.dsr2.2009.09.007.

Figueiras, F.G., Teixeira, I.G., Froján, M., Zúñiga, D., Arbones, B., Castro, C.G., 2020. Seasonal Variability in the Microbial Plankton Community in a Semienclosed Bay Affected by Upwelling: The Role of a Nutrient Trap. Front. Mar. Sci. 7, 578042. doi: 10.3389/fmars.2020.578042.

Fraga, S., 1989. Las purgas de mar en las Rías Bajas gallegas. In: Fraga F, Figueiras FG (eds) Las purgas de mar como fenómeno natural. Las mareas rojas. Cuadernos da Área de Ciencias Mariñas, Seminario de Estudos Galegos 4, p 95-109.

Fritz, L., Triemer, R.E., 1985. A rapid simple technique utilizing calcofluor white M2R for the visualization of dinoflagellate thecal plates. J. Phycol. 21, 662–664. https://doi.org/10.1111/j.0022-3646.1985.00662.x.

Garcés, E., Bravo, I., Vila, M., Figueroa, R.I., Masó, M., Sampedro, N., 2004. Relationship between vegetative cells and cyst production during *Alexandrium minutum* bloom in Arenys de Mar harbour (NW Mediterranean). J. Plankton Res. 26, 637–645. https://doi.org/10.1093/plankt/fbh065.

Gessner, B.D., 2000. Impact of toxic episodes: neurotoxic toxins. In: Botana, L.M. (Ed.), Seafood and Freshwater Toxins. Pharmacology, Physiology and Detection. Marcel Dekker Inc, New York Basel, pp. 65–90.

Giacobbe, M.G., Oliva, F.D., Maimone, G., 1996. Environmental factors and seasonal occurrence of the dinoflagellate *Alexandrium minutum*, a PSP potential producer, in a mediterranean lagoon. Estuar. Coast. Shelf Sci. 42, 539–549. https://doi.org/10.1006/ecss.1996.0035.

Gimeno, L., Trigo, R.M., Gómez-Gesteira, M., 2011. Regional climate change in the NW Iberian Peninsula. Clim Res 48:105-108. doi: 10.3354/cr01017.

Gladan, Z.N., Matić, F., Arapov, J., Skejić, S., Bužančić, M., Bakrač, A., Straka, M., Dekneudt, Q., Grbec, B., Garber, R., Nazlić, N., 2020. The relationship between toxic phytoplankton species occurrence and environmental and meteorological factors along the Eastern Adriatic coast. Harmful Algae 92, 101745–101761. https://doi.org/10.1016/j.hal.2020.101745.

Gobler, C.J., Doherty, O.M., Hattenrath-Lehmann, T.K., Griffith, A.W., Kang, Y., Litaker, R., 2017. Ocean warming since 1982 has expanded the niche of toxic algal blooms in the North Atlantic and North Pacific oceans. PNAS 114, 4975–4980. https://doi.org/10.1073/pnas.1619575114.

Gómez-Gesteira, M., Montero, P., Prego, R., Taboada, J.J., Leitão, P., Ruiz-Villarreal, M., Neves, R., Perez-Villar, V., 1999. A two-dimensional particle tracking model for pollution dispersion in A Coruña and Vigo Rias (NW Spain). Oceanol. Acta 22, 167–177. https://doi.org/10.1016/S0399-1784(99)80043-7.

Gómez-Gesteira, M., Gimeno, L., de Castro, M., Lorenzo, M.N., Alvarez, I., Nieto, R., Taboada, J.J., Crespo, A.J.C., Ramos, A.M., Iglesias, I., Gómez-Gesteira, J.L., Santo, F.E., Barriopedro, D., Trigo, I.F., 2011. The state of Climate in NW Iberia. Clim. Res. 48, 109–144. https://doi.org/10.3354/CR00967.

Guallar, C., Bacher, C., Chapelle, A., 2017. Global and local factors driving the phenology of *Alexandrium minutum* (Halim) blooms and its toxicity. Harmful Algae 67, 44–60. https://doi.org/10.1016/j.hal.2017.05.005.

Guerrero-Feijóo, E., Nieto-Cid, M., Dobal-Amador, V., Hernando-Morales, V., Sintes, E., Álvarez, M., Balagué, V., Varela, M.M., 2017. Optical properties of disolved organic matter relate to different depth-specific patterns of archaeal and bacterial community structure in the north Atlantic ocean. FEMS Microbiol. Ecol. 93, 1–14. https://doi.org/10.1093/femsec/fiw224.

Guillard, R.R.L., Hargraves, P.E., 1993. *Stichochrysis immobilis* is a diatom, not a chrysophyte. Phycologia 32, 234–236. https://doi.org/10.2216/i0031-8884-32-3-234.1.

Guillou, L., Bachar, D., Audic, S., Bass, D., Berney, C., Bittner, L., Boutte, C., Burgaud, G., de Vargas, C., Decelle, J., Del Campo, J., Dolan, J.R., Dunthorn, M., Edvardsen, B., Holzmann, M., Kooistra, W.H., Lara, E., Le Bescot, N., Logares, R., Mahé, F., Massana, R., Montresor, M., Morard, R., Not, F., Pawlowski. J., Probert, I., Sauvadet, A.L., Siano, R., Stoeck, T., Vaulot, D., Zimmermann, P., Christen, R., 2013. The Protist Ribosomal Reference database (PR2): a catalog of unicellular eukaryote small sub-unit rRNA sequences with curated taxonomy. Nucleic Acids Res. 41(Database issue), D597-604. doi: 10.1093/nar/gks1160.

Hallegraeff, G.M., 2010. Ocean climate change, phytoplankton community responses, and harmful algal blooms: a formidable predictive challenge. J. Phycol. 46, 220–235. https://doi.org/10.1111/j.1529-8817.2010.00815.x.

Hallegraeff, G.M., Anderson, D.A., Belin, C., Decharoui Bottein, M.-Y., Bresnan, E., Chinain, M., Enevoldsen, H., Iwataki, M., Karlson, B., McKenzie, C.H., Sunesen, I., Pitcher, G.C., Provoost, P., Richardson, A., Scheibold, L., Tester, P.A., Trainer, V.L., Yñiguez, A.T., Zingone, A., 2021. Perceived global increase in algal blooms is

attributable to intensified monitoring and emerging bloom impacts. Comm. Earth Environ. 2, 117. https://doi.org/10.1038/s43247-021-00178-8.
Huhn, F., Kameke, A., Allen-Perkin, S.S., Montero, P., Venancio, A., Pérez-Muñuzuri, V., 2012. Horizontal Lagrangian transport in a tidal-driven estuary—Transport barriers attached to prominent coastal boundaries. Cont. Shelf Res. 39, 1–13. https://doi.org/10.1016/j.csr.2012.03.005.
Ki, J.S., Han, M.S., 2007. Informative characteristics of 12 divergent domains in complete large subunit rDNA sequences from the harmful dinoflagellate genus, *Alexandrium* (Dinophyceae). J. Eukaryot. Microbiol. 54, 210–219. https://doi.org/10.1111/j.1550-7408.2007.00251.x.
Klose, K., Cooper, S.D., Bennett, D.M., 2015. Effects of wildfire on stream algal abundance, community structure, and nutrient limitation. Freshw. Sci. 34, 1494–1509. https://doi.org/10.1086/683431.
Kotob, S.I., McLaughlin, S.M., Van Berkum, P., Faisal, M., 1999. Discrimination between two *Perkinsus* spp. isolated from the softshell clam, *Mya arenaria*, by sequence analysis of two internal transcribed spacer regions and the 5.8S ribosomal RNA gene. Parasitology 119, 363–368. https://doi.org/10.1017/s0031182099004801.
Ladd, T.M., Ramírez Negrón, A., Kim, S.M., Iglesias-Rodríguez, D., 2020.dfire Ash Promotes Growth of Santa Barbara Channel Phytoplankton Communities Under Low Nutrient Conditions. Oral communication Ocean Sciences Meeting, San Diego (CA), February 2020. https://agu.confex.com/agu/osm20/preliminaryview.cgi/Paper636175.html.
Langmann, B., Zaksek, K., Hort, M., Duggen, S., 2010. Volcanic ash as fertiliser for the surface ocean. Atmos. Chem. Phys. 10, 3891–3899. https://doi.org/10.5194/acp-10-3891-2010.
Lau, W.L.S., Law, I.K., Liow, G.R., Hii, K.S., Usup, G., Lim, P.T., Leaw, C.P., 2017. Life-history stages of natural bloom populations and the bloom dynamics of a tropical Asian ribotype of *Alexandrium minutum*. Harmful Algae 70, 52–63. https://doi.org/10.1016/j.hal.2017.10.006.
Leitão, P., 1996. Modelo de dispersão lagrangeano tridimensional [Tridimensional model of lagrangian dispersion]. M.D. Thesis. IST. Lisboa.
Lewis, A.M., Coates, L.N., Turner, A.D., Percy, L., Lewis, J., Mock, T., 2018. A review of the global distribution of *Alexandrium minutum* (Dinophyceae) and comments on ecology and associated paralytic shellfish toxin profiles, with a focus on Northern Europe. J. Phycol. 54 (5), 581–598.
Lindahl, O., 1986. A dividable hose for phytoplankton sampling, Vol. 26. International Council for the Exploration of the Sea, Center of Environmental Science (Annex 3).
Lourido, A., Moreira, J., Troncoso, J.S., 2010. Spatial distribution of benthic macrofauna in subtidal sediments of the Ría de Aldán (Galicia, northwest Spain). Sci. Mar. 74 (4), 705–715.
Maguer, J., Wafar, M., Madec, C., Morin, P., Denn, E., 2004. Nitrogen and phosphorus requirements of an *Alexandrium minutum* bloom in the Penzé Estuary, France. Limnol. Oceanogr. 49, 1108–1114. https://doi.org/10.4319/lo.2004.49.4.1108.
Margalef, R., 1956. Estructura y dinámica de la Purga de Mar en la Ría de Vigo. Inv. Pesq. 5, 113–134.
Martin, M., 2011. Cutadapt removes adapter sequences from high-throughput sequencing reads. EMBnet.journal 17 (1), 10–12. https://doi.org/10.14806/ej.17.1.200.
Martins, F., Leitão, P., Silva, A., Neves, R., 2001. 3D modelling in the Sado estuary using a new generic vertical discretization approach. Oceanol. Acta 24, 51–62. https://doi.org/10.1016/S0399-1784(01)00092-5.
Massana, R., Murray, A.E., Preston, C.M., DeLong, E.F., Veth, C., Pernthaler, A., Pernthaler, J., 1997. Vertical distribution and phylogenetic characterization of marine planktonic Archaea in the Santa Barbara Channel. Appl. Environ. Microbiol. 63, 50–56. https://doi.org/10.1128/aem.63.1.50-56.1997.
Memoria sobre el estado de las obras del Puerto de Vigo en 31 de diciembre de 1926 — Vigo: Junta de Obras del Puerto, 1927.
Meteogalicia, 2018. Monthly report of environmental conditions for June 2018. Xunta de Galicia. Consellería de Medio Ambiente e Ordenación do Territorio, p 29.
Morgan, S.G., Fisher, J.L., 2010. Larval behaviour regulates nearshore retention and offshore migration in an upwelling shawow and along the open coast. Mar. Ecol. Prog. Ser. 404, 109–126. https://doi.org/10.3354/meps08476.
Morien, E., Parfrey, L.W., 2018. SILVA v128 and v132 dada2 formatted 18s 'train sets' (Version 1.0). Zenodo. https://zenodo.org/record/1447330#.YiHGbejMLcs.
Nascimento, S.M., Mendes, M.C.Q., Menezes, M., Rodríguez, F., Alves-de-Souza, C., Branco, S., Riobó, P., Franco, J., Nunes, J.M.C., Huk, M., Morris, S., Fraga, S., 2017. Morphology and phylogeny of *Prorocentrum caipirignum* sp. *nov*. (Dinophyceae), a new tropical toxic benthic dinoflagellate. Harmful Algae 70, 73–89. https://doi.org/10.1016/j.hal.2017.11.001.
Pérez, F.F., Padín, X.A., Pazos, Y., Gilcoto, M., Cabanas, M., Pardo, P.C., Doval, D., Farina-Busto, L., 2010. Plankton response to weakening of the Iberian coastal upwelling. Glob. Change Biol. 16 (4), 1258–1267. https://doi.org/10.1111/j.1365-2486.2009.02125.x.
Piredda, R., Tomasino, M.P., D'Erchia, A.M., Manzari, C., Pesole, G., Montresor, M., Kooistra, W.H.C.F., Sarno, D., Zingone, A., 2017. Diversity and temporal patterns of planktonic protest assemblages at a Mediterranean Long Term Ecological Research site. FEMS Microbiol. Ecol. 93, fiw200. https://doi.org/10.1093/femsec/fiw200.
R Core Team, 2020. R: A Language and Environment for Statistical Computing. R Foundation for Statistical Computing, Vienna, Austria https://www.R-project.org/.
Reguera, B., Escalera, L., Pazos-González, Y., Moroño, A., 2008. Episodios de fitoplancton tóxico en la Ría de Vigo. In: González-Garcés, A., Vilas-Martín, F., Álvarez-Salgado, X.A. (eds) La Ría de Vigo. Una aproximación integral al ecosistema marino de la Ría de Vigo. Instituto de Estudios Vigueses, p 153-199.
Rodríguez, F., 2017. Mareas vermellas en Galicia: mitos e realidade. Boletín do Instituto de Estudios Vigueses 22, 313–340.
Rodríguez, F., Garrido, J.L., Llewellyn, C.A., 2020. Photosynthetic pigments in dinoflagellates. In: Dinoflagellates: classification, evolution, physiology and ecological significance. Subba Rao V. Durvasula (Ed.). Nova Science Publishers, Inc. New York. 39-61 pp.
Rodríguez, F., Pazos, Y., Maneiro, J., Zapata, M., 2003. Temporal variation in phytoplankton assemblages and pigment composition in a fixed station of the Ría of Pontevedra (NW Spain). Estuar. Coast. Shelf Sci. 58, 499–515. https://doi.org/10.1016/S0272-7714(03)00130-6.
Ryan, J.P., McManus, M.A., Kudela, R.M., Lara-Artigas, M., Bellingham, J.G., Chavez, F. P., Doucette, G., Foley, D., Godin, M., Harvey, J.B.J., Marin III, R., Messié, M., Mikulski, C., Pennington, T., Py, F., Rajan, K., Shulman, I., Wang, Z., Zhang, Y., 2014. Boundary influences on HAB phytoplankton ecology in a stratification-enhanced upwelling shadow. Deep Sea Res. Part II Top. Stud. Oceanogr. 101, 63–79. https://doi.org/10.1016/j.dsr2.2013.01.017.
Santos, M., Reis Costa, P., Porteiro, F.M., Moita, M.T., 2014. First report of a massive bloom of *Alexandrium minutum* (Dinophyceae) in middle North Atlantic: A coastal lagoon in S.Jorge Island. Azores. Toxicon 90, 265–268. https://doi.org/10.1016/j.toxicon.2014.08.065.
Silins, U., Bladon, K.D., Kelly, E.N., Esch, E., Spence, J.R., Stone, M., Emelko, M.B., Boon, S., Wagner, M.J., Williams, C.H.S., Tichkowsky, I., 2014. Five-year legacy of wildfire and salvage logging impacts on nutrient runoff and aquatic plant, invertebrate, and fish productivity. Ecohydrol 7, 1508–1523. https://doi.org/10.1002/eco.1474.
Sobrino, R., 1918. La purga del mar o hematotalasia. Mem. R. Soc. Esp. Hist. Nat. 10, 407–458.
Sousa, M.C., Ribeiro, A., Des, M., Gomez-Gesteira, M., de Castro, M., Dias, J.M., 2020. NW Iberian Peninsula coastal upwelling future weakening: Competition between wind intensification and surface heating. Sci. Total Environ. 703, 134808. doi: 10.1016/j.scitotenv.2019.134808.
Stock, C.A., McGillicuddy, D.J., Solow, A.R., Anderson, D.M., 2005. Evaluating hypotheses for the initiation and development of *Alexandrium fundyense* blooms in the western Gulf of Maine using a coupled physical-biological model. Deep Sea Res. Part II Top. Stud. Oceanogr. 52, 2715-2744. doi: 10.1016%2Fj.dsr2.2005.06.022.
Stoeck, T., Bass, D., Nebel, M., Christen, R., Jones, M.D.M., Breiner, H.-W., Richards, T. A., 2010. Multiple marker parallel tag environmental DNA sequencing reveals a highly complex eukaryotic community in marine anoxic water. Mol. Ecol. 19, 21–31. https://doi.org/10.1111/j.1365-294X.2009.04480.x.
Tang, W., Llort, J., Weis, J., Perron, M.M.G., Basart, S., Li, Z., Sathyendranath, S., Jackson, T., Sanz-Rodríguez, E., Proemse, B.C., Bowie, A.R., Schallenberg, C., Strutton, P.G., Matear, R., Cassar, N., 2021. Widespread phytoplankton blooms triggered by 2019–2020 Australian wildfires. Nature 597, 370–375. https://doi.org/10.1038/s41586-021-03805-8.
Tester, P.A., Litaker, R.W., Berdalet, E., 2020. Climate change and harmful benthic microalgae. Harmful Algae 91, 101655. https://doi.org/10.1016/j.hal.2019.101655.
Venâncio, A., Montero, P., Costa, P., Regueiro, S., Brands, S., Taboada, J., 2019. An Integrated Perspective of the Operational Forecasting System in Rías Baixas (Galicia, Spain) with Observational Data and End-Users. In: Rodrigues, J. et al. (eds) Computational Science – ICCS 2019. Lecture Notes in Computer Science, 11539.
Vicente-Serrano, S.M., López-Moreno, J.I., Drumond, A., Gimeno, L., Nieto, R., Morán-Tejeda, E., Lorenzo-Lacruz, J., Beguería, S., Zabalza, J., 2011. Effects of warming processes on droughts and water resources of the NW Iberian Peninsula (1930–2006). Clim. Res. 48, 203–212. https://doi.org/10.3354/cr01002.
Vila, M., Masó, M., 2005. Phytoplankton functional groups and harmful algal species in anthropogenically impacted waters of the NW Mediterranean Sea. Sci Mar 69, 31-45. doi: 10.3989/scimar.2005.69n131.
Wells, M.L., Karlson, B., Wulff, A., Kudela, R., Trick, C., Asnaghi, V., Berdalet, E., Cochlan, W., Davidson, K., De Rijcke, M., Dutkiewicz, S., Hallegraeff, G., Flynn, K.J., Legrand, C., Paerl, H., Silke, J., Suikkanen, S., Thompson, P., Trainer, V.L., 2020. Future HAB science: directions and challenges in a changing climate. Harmful Alga 91, 101632. https://doi.org/10.1016/j.hal.2019.101632.
Zapata, M., Rodríguez, F., Garrido, J.L., 2000. Separation of chlorophylls and carotenoids from marine phytoplankton: a new HPLC method using a reversed phase C8 column and pyridine-containing mobile phases. Mar. Ecol. Prog. Ser. 195, 29–45. https://doi.org/10.3354/meps195029.